Rep. Prog. Phys., Vol. 44, 1981. Printed in Great Britain

Potentials of surfaces in space

Elden C Whipple

Center for Astrophysics and Space Science, University of California at San Diego, La Jolla, California 92093, USA

Abstract

In the last decade, large electrostatic potentials of the order of tens of kV have been measured on spacecraft in the Earth's magnetosphere. Observations in space have led to the inference of large potentials on natural objects in the solar system. The result for spacecraft can be material damage and operational interference caused by electrostatic discharges. Natural objects such as dust grains can be disrupted, and their motion influenced by electromagnetic forces.

The potential of a body in space is determined by a balance between various charging currents. The most important are transfer of charge from plasma particles, photoemission, and secondary electron emission, with other charging mechanisms sometimes contributing. The currents are affected by the body's charge and motion and by local magnetic and electric fields. Dielectric surfaces may have surface potential gradients which can affect the current balance through the creation of potential barriers.

These processes are evaluated for bodies in the solar system and in interstellar space. Expected equilibrium potentials range from a few tenths of a volt negative in the ionosphere to a few volts positive in the quiet magnetosphere and in interplanetary space. However, large negative potentials can occur in hot plasmas such as in the disturbed magnetosphere, especially on shaded surfaces. Potentials in interstellar space can be positive or negative, depending on the properties of the local radiation field and plasma.

In regions where there have been measurements of spacecraft potentials the results generally agree with these expectations. Deviations can be attributed to the effects of biased or dielectric surfaces or to the magnetic induction effect in large structures such as antennae. An intensive research effort has been initiated to measure material properties, to study charging and discharge processes, to model the current balance to realistic spacecraft configurations, and to obtain additional data in space. Spacecraft potential control experiments have been carried out using passive methods, such as careful surface material selection, and active methods, such as emission of charged-particle beams.

The review closes with a survey of possible astrophysical applications where charging effects may be important.

This review was received in March 1981.

0034-4885/81/111197+56 $06.50

Contents

1. An overview of charging

1.1. Introduction

Consider a body in space that is small enough such that it has no significant atmosphere of its own, such as a dust grain, an asteroid or a spacecraft. Its surface is then exposed to the space environment and is continually being bombarded by incident charged particles and photons. The sticking coefficient for electrons on a solid surface is essentially unity for low electron energies. Low-energy ions pull an electron out of the solid material by field emission when they get within a few ångströms of the surface and then go off as neutral atoms. At higher energies, above tens of eV for electrons and tens of keV for ions, secondary electron emission processes are important. Incident energetic photons can cause the emission of photoelectrons. All of these processes are mechanisms for charge transfer between the body and its environment.

The rate at which charge transfer proceeds depends both upon characteristics of the body and on the environmental conditions. In particular, the rate of charge transfer depends on the charge already residing on the body. That is, the motion of charged particles in the vicinity of the body is influenced by the electric field arising from the distributed charge. For example, a positive charge will attract electrons and repel ions, and secondary or photoelectrons may not escape but may return to the body. Charge transfer will proceed until an equilibrium is reached when the net current to the surface vanishes. In general, this equilibrium charge will not be zero. In a plasma where emission processes are unimportant the equilibrium charge will be negative because of the higher flux of electrons to an uncharged surface compared to ions. In regions where photoemission is the dominant process, the equilibrium charge will be positive.

Knowledge of the equilibrium charge on a body is important to a number of areas of investigation. In certain regions of interstellar space the flux of ions and electrons to dust grains constitutes a significant loss mechanism for the charged particles in the medium. Photoemission from grains can at times be a significant source of kinetic energy for the interstellar gas. Knowledge of the grain's charge is necessary to evaluate both of these processes. In the solar system, the motion of charged dust grains is affected by the magnetic and electric fields of the solar wind and also by the fields local to the planets and their satellites.

A negatively charged spacecraft has an increased drag in the Earth's ionosphere because of its larger cross section for momentum transfer to positive ions. Plasma waves may be excited by the motion of a charged spacecraft and carry away energy. The electric charge on a spacecraft is especially important in its effect on experiments designed to measure the properties of charged particles and electric fields in the environment. The interpretation of data from such experiments must take into account the effects of the vehicle charge. Conversely, the charge may be determined from the characteristics of the data.

1.2. Recent observations

There has been heightened interest in the subject of the electric charge on bodies in space in the last decade as a result of a number of space experiments. The most spectacular of these was the observation by DeForest (1972, 1973) that the ATS-5 spacecraft in the

Earth's magnetosphere at times attained negative potentials of several kilovolts. A record potential of -19 kV was observed on ATS-6 (Olsen and Purvis 1981). The largest potentials were observed during times of magnetic activity as these synchronous-orbit spacecraft entered the Earth's shadow. In quiet conditions, the equilibrium potential of a spacecraft at synchronous orbit (6.6 Earth radii) is of the order of a few volts positive as the result of a balance between photoemission and charged-particle collection. However, during magnetic storms, the electron temperature can at times approach 10^4 eV (10^8 K) at these altitudes, and when the photoemission current vanishes as eclipse is entered, the spacecraft charges up to a negative potential roughly equivalent to the electron temperature (i.e. $kT/e = 10$ kV).

At about the same time as these initial observations of large spacecraft potentials, a number of unexplained spacecraft anomalies and the operational loss of one synchronous satellite were reported. It was quickly realised that large differential potentials between different portions of a spacecraft surface could lead to electric discharges and associated material damage. Several studies of anomalous behaviour of spacecraft systems (Fredricks and Scarf 1973, Pike and Bunn 1976) showed that the anomalies correlated well with charging on spacecraft (Reasoner *et al* 1976). These events have led to a vigorous research programme involving laboratory work on material properties and charging and discharge processes, the development of computational techniques for estimating the charging of realistic spacecraft configurations, and the launching of a research spacecraft in January 1979 to study 'Spacecraft Charging at High Altitude' with the acronym 'SCATHA' (McPherson *et al* 1975, McPherson and Schober 1976, Lovell *et al* 1976, Durrett and Stevens 1979).

In addition to the direct evidence for spacecraft charging, there have been a number of observations which have indirectly emphasised the importance of charging of natural objects in the solar system. There had been previous speculation that charging of dust grains on the lunar surface might lead to electrostatic transport of the lunar surface material (e.g. Gold 1955, Singer and Walker 1962b). The crew of Apollo 17 at an altitude of 100 km above the Moon saw streamers accompanying spacecraft sunrise, probably produced by light scattered from particulates extending from the lunar surface to above the spacecraft (McCoy and Criswell 1974). Criswell (1973) and Rennilson and Criswell (1974) reported horizon glow observed from the Surveyor 5, 6 and 7 spacecraft on the lunar surface following sunset. Both of these observations might be explained by electrostatic 'levitation' of dust grains. Plasma measurements by experiments on the lunar surface have inferred the lunar surface potential and electric field (e.g. Reasoner and Burke 1972, 1973). The role of Jupiter's satellite Io in modulating the decametric emissions from Jupiter's magnetosphere may involve large potential differences across Io's sheath to the magnetosphere or across Io itself (Gurnett 1972, Shawhan *et al* 1973). More recently, Fechtig *et al* (1979) reported that micrometeoroid observations near the Earth frequently occur in bursts. They infer that 'swarms' of particles, which occur only within 10 Earth radii, are produced by electrostatic disruption of larger bodies as they pass through the Earth's auroral zones. The recent observations by Voyager of 'spokes' and 'braids' in Saturn's rings are striking evidence for forces other than gravity acting on the ring particles. Electric and magnetic forces acting on charged dust grains are the most likely candidates for these additional forces.

1.3. Charge, potential, capacitance and sheaths

It is usually more convenient to discuss the charge on a body in terms of the corresponding potential with respect to the surrounding medium. The charging currents to a body depend

on the body's potential rather than charge; also, the potential is the quantity more easily inferred from measurements. The relation between the charge and potential involves the body's capacitance which, in general, is a strong function of the environment. As a simple example, consider Poisson's equation in spherical coordinates for the potential φ, where the space charge ρ around a sphere is given by

$$\rho = n_0 e[1 - \exp(\varphi e/kT)]. \tag{1.1}$$

Here, n_0 is the unperturbed ion or electron density, e is the elementary charge, k is Boltzmann's constant and T is the electron temperature. The first term gives the approximate ion density and the second the electron density in front of a fast moving spherical body with a negative potential φ_s. This neglects wake effects and assumes that the ion streaming energy is large enough that the ions are not deflected by the potential distribution. Poisson's equation may then be written approximately as

$$\frac{d^2\varphi}{dr^2} + \frac{2}{r}\frac{d\varphi}{dr} \cong \frac{n_0 e}{\varepsilon_0}\left(\frac{\varphi e}{kT}\right) \tag{1.2}$$

where ε_0 is the permittivity.

The solution of (1.2) is the well-known Debye potential:

$$\varphi = \varphi_s \frac{R}{r} \exp[-(r-R)/L] \tag{1.3}$$

where R is the body radius and L is the Debye length:

$$L = (\varepsilon_0 kT/n_0 e^2)^{1/2}. \tag{1.4}$$

The capacitance of the body in the plasma may be obtained from the ratio of the charge on the body to its potential and is given by

$$C = 4\pi R^2 \varepsilon_0 \left(\frac{1}{R} + \frac{1}{L}\right). \tag{1.5}$$

This is simply the capacitance for two concentric spheres with a separation distance L. Thus the Debye length gives the approximate screening distance or sheath thickness about a charged body in a plasma. In space, the Debye length varies from a few millimetres in the ionosphere to tens and hundreds of metres in the magnetosphere and interplanetary space, perhaps reaching values as large as a few kilometres in low-density interstellar regions.

The size of a body compared to the Debye length is a useful criterion for deciding whether or not sheath effects must be taken into account in evaluating the charging currents to a body. A body small with respect to the Debye length is essentially unshielded and Laplace's equation without space charge may be used to obtain the local potential distribution. Bodies of the order of or larger than the Debye length have a space charge sheath which may have to be evaluated in order to obtain the currents. This can be a difficult problem since it involves the self-consistent solution of Poisson's equation for the potential distribution and the Vlasov equation for the particle distribution functions.

1.4. Outline of sections

This paper reviews the subject of surface potentials in space with an emphasis on developments in the last decade. Section 2 gives a historical survey of work up until the early

1970s. Other reviews and collections of papers may be found in Singer (1965), Kasha (1969), Grard (1973a), Rosen (1976), and in the proceedings of the three biannual conferences on spacecraft charging and technology (Pike and Lovell 1977, Finke and Pike 1979, Pike and Stevens 1981). Topical reviews devoted to particular aspects of charging will be referred to at appropriate places in the discussion.

Section 3 contains a discussion of the various charging mechanisms. The effects of non-isotropic plasmas, wakes and environmental magnetic and electric fields are discussed in §4. The concept of equilibrium potential, its stability, time constants for charging, and expected potentials in various regimes are covered in §5. Section 6 describes differential charging, potential barriers and discharge processes. Section 7 reviews measurements of spacecraft potentials. Recent work on potential modification and control on spacecraft is discussed in §8. Section 9 describes astrophysical applications where charging effects on bodies may be important. Finally, §10 concludes with a summary of the main advances and indicates where further work is needed.

2. Survey of early work on charging

2.1. Astrophysical work

Apparently the first paper to treat the problem of charging of bodies in space was by Jung (1937). He obtained equations for fluxes of ions and electrons to an interstellar grain and concluded that photoemission and electron accretion were the dominant processes; he found equilibrium potentials of one to a few volts positive. Spitzer (1941) showed that negative potentials of about -2 V would be realised for grains in H II regions. The effects of dust in 'de-ionising', i.e. providing a recombination surface for the plasma, was mentioned but not discussed in detail. Cernuschi (1947) considered the effects of varying sticking probabilities for the electrons on grains consisting of dielectric substances. Spitzer (1948) and Spitzer and Savedoff (1950) treated in some detail the charge collection and emission processes for grains. They pointed out that field emission would limit the negative potentials of small grains. Photosensitive or metallic grains might have positive potentials up to about 10 V in regions where photoemission was important.

Whipple (1940, 1960) suggested that meteoroids in interplanetary space must carry a positive charge due to the photoelectric effect and hence would be subjected to perturbations in their orbits by the solar magnetic field. The charging of grains in the solar system is a key element in Alfven's ideas concerning the origin of the solar system (1954). A negative charge on the grain enhances the flux of positive ions to its surface; a finite sticking probability will cause the grains to grow in size, leading to a condensation of the ionised material. The magnetic and electrical forces acting on the grains lead to a mass distribution in the equatorial plane of the central body which Alfven compared to both the Saturn ring distribution and the asteroid distribution. Singer (1956) and Opik (1957) looked at the charge on dust near the Earth and concluded that the capture rate of dust by the Earth would not be significantly enhanced by the effects of the Earth's magnetic field on the particle's motion; Opik pointed out that electrostatic disruption could limit the size of small grains. Singer and Walker (1962a) showed that photoelectric screening of grains was negligible but could be significant for larger bodies (see also Walbridge 1969). Shen and Chopra (1963) considered the effects of thermionic emission for a body in a plasma near the Sun, or any hot star, and worked out the screening distance for the charge in the plasma. Parker (1964) discussed the perturbation of charged dust grains

by the electric and magnetic fields of the solar wind. The fluctuating direction of the magnetic field tends to take small grains away from the ecliptic. Peale (1966) and Shapiro *et al* (1966) looked at the effect of charge on dust grains in connection with the possibility of a dust belt about the Earth and showed that the electric and magnetic forces were small compared to other influences. Reviews which discuss the work on charge on interplanetary dust grains up through this period of time are contained in Belton (1966), Vedder (1966) and Wyatt (1969).

In addition to the work on charging of interplanetary grains, there were also predictions of charging of the lunar surface dust. Gold (1955, 1961, 1962) suggested that electrical charging of the dust on the Moon could lead to its surface transport and thus help to explain apparent erosion. Opik and Singer (1960) and Opik (1962) argued that photoemission would charge the Moon to about +20 V and the resulting electric field could accelerate the escape of heavy atoms because of their eventual ionisation. They treated the Moon as a conductor at one potential. This work was extended by Grobman and Blank (1969) who calculated the surface potential as a function of solar zenith angle and found potentials varying from about +3 V at the subsolar point to less than 1 V at the limb. Singer and Walker (1962b) showed that the potential of a grain on the lunar surface is different from that of an isolated grain in space because the currents are determined by the macroscopic electric field; the charge on a grain should be proportional to the grain's area and the lunar surface electric field.

2.2. Early work on spacecraft charging

The advent of spaceflight in the late 1950s stimulated a great amount of theoretical work on the possible electrical interactions between a spacecraft and its environment. Most of the physical processes that had been considered for the charging of dust grains in space could equally as well apply to a large body such as a spacecraft. The major difference had to do with the fact that since the early spacecraft were at ionospheric altitudes, the high electron densities meant shielding effects of the plasma sheath had to be taken into account. Also, satellite velocities in the ionosphere were larger than the ion thermal velocity but smaller than the electron thermal velocity. Consequently, the ion current to a spacecraft at these altitudes was largely determined by the sweeping-up effect of the fast-moving satellite in its motion through the plasma.

The first calculation of the charge on a macroscopic body was apparently made by Lehnert (1956) in anticipation of the orbiting of Earth satellites. He took into account the increased positive-ion current on the satellite's forward surface due to the high satellite to ion velocity ratio. The resulting potential obtained by balancing this against the electron current was about −0.7 to −1.0 V. Photoemission could change this value, depending on the surface material. He discussed the increased ion drag and the possibility of the excitation of plasma oscillations. In an important paper, Jastrow and Pearse (1957) calculated the potential, screening distance and ion drag of a satellite. The potentials they obtained of −20 to −60 V were large compared with later measurements because they used too high an electron temperature, but the paper stimulated a great deal of interest in the community of scientists just getting involved in space exploration.

In anticipation of the first Soviet Sputnik, Gringauz and Zelikman (1957) discussed the distribution of charged particles around a satellite and derived an expression for the equilibrium potential, taking into account the satellite's velocity and photoemission. Imyanitov (1957) discussed the problems of measuring an electric field in the ionosphere from a satellite. The field due to the charge on the satellite must be taken into account.

Its magnitude was estimated at several V cm^{-1} by computing the satellite potential in a manner similar to that of Gringauz and Zelikman and estimating the sheath thickness from plasma probe theory. Chang and Smith (1959) also derived an expression for satellite potential by balancing a simple ram expression plus a first-order correction for the ion current against the electron current. Beard and Johnson (1960) discussed the interaction of a satellite with the Earth's magnetic field. The induced potential gradient could be as high as 0.2 V m^{-1}; this would affect the distribution of the electron flow to the satellite surface and also the measurement of satellite potential. Beard and Johnson (1961) also discussed the possibility of attaining large satellite potentials by emitting a beam of charged particles. Higher negative than positive potentials would be possible because of the limited mobility of the plasma positive ions constituting the return current.

Chopra in a review article (1961) obtained expressions for a body at rest or in motion. He observed that the photoelectric effect would be important at higher altitudes in the Earth's atmosphere. Kurt and Moroz (1962) predicted positive potentials up to +4 V above altitudes where the electron density was about 300 cm^{-3}. They suggested that large negative potentials of several kilovolts might be possible in regions of high concentrations of energetic electrons, as in the outer radiation zone. Rawer (1963) evaluated the effects of photoemission by considering recent values for the solar flux in the ultraviolet part of the spectrum and photoelectric yields for typical materials. He pointed out that in regions of low electron density the satellite potential might be determined by strong emission lines such as the hydrogen Lyman alpha line.

The question of the perturbation of the plasma environment by a spacecraft moving through it at a high speed received a great deal of early theoretical attention. In addition to the sheath about the spacecraft, it was recognised that there would be a region behind the spacecraft that would be depleted of positive ions—a space charge wake. The wake would be negative because electrons could more easily fill in the depleted region. Determination of the structure of the wake involves the simultaneous treatment of Poisson's equation for the potential distribution and a calculation of the effects of the wake on the charged-particle motion in the disturbed region, with appropriate boundary conditions. Several groups were especially prominent in attacking this problem of the distribution of charged particles around a satellite, especially in Russia. Reviews of the Russian work may be found in Al'pert *et al* (1963), Al'pert (1965) and Gurevich *et al* (1969). The work in the United States was partially stimulated by the apparent observation of radio echoes from disturbed plasma regions near satellites as they crossed the sky overhead (e.g. Kraus 1965). Groups at the University of Maryland (Walker 1964, 1965, Bettinger 1964, Opik 1965) and at the University of Michigan (Chen 1965, Liu and Hung 1968, Liu and Jew 1968, Liu 1969) made contributions. Other workers during this period were Davis and Harris (1961), Parker (1964), Taylor (1967) and Call (1969), with the various treatments differing primarily in how the complicated particle trajectory problem was handled. Reviews of these approaches to solving the Poisson–Vlasov equations have been given by Parker (1976a) and Whipple (1977). Drell *et al* (1965a, b) suggested that the moving spacecraft could excite Alfven waves through the $\boldsymbol{V} \times \boldsymbol{B}$ effect and cause increased drag, but this phenomenon has never been verified.

3. Charging processes

3.1. Collection of plasma particles

The current density to any point on the surface of a body in a plasma is given by an

integral over the particle distribution function for a given species of particle and a summation over species. The integral expression for one species is

$$J=q\int\int\int v_s \cos\theta f(v_s)\,\mathrm{d}^3v_s \tag{3.1}$$

where the subscript 's' refers to the fact that the velocity is the local velocity at the surface of the body. The particle charge is given by q, θ is the angle of v_s from the surface normal, and f is the distribution function. There are two steps involved in evaluating this integral: first, the distribution function of the particles at the surface must be determined; and second, the limits on the integral must be determined. For a current consisting of particles from an isotropic plasma where the distribution depends only on the speed, or equivalently on the particle kinetic energy, the distribution function at the surface can be obtained immediately from conservation of energy. Consequently, for an isotropic plasma it is only the determination of the limits of the integral that may be a problem.

In the general case where sheath effects may be important or where the body has an irregular shape, it is necessary to examine particle trajectories in order to find the limits for the integral, even when the plasma itself is isotropic. A useful concept that can be applied to bodies with certain kinds of symmetries is the distinction between 'orbit-limited current' and 'sheath-limited current'. Orbit-limited currents are conventionally defined as the largest currents, as functions of the potential, that can be collected by perfectly absorbing spherical or infinite cylindrical bodies from a collisionless, stationary, isotropic plasma. Orbit-limited behaviour prevails when all positive-energy orbits ending on the body actually connect back to infinity in the plasma. Thus a repulsive potential which decreases monotonically outwards from a convex surface always results in an orbit-limited current. For an attractive potential, it can be shown that orbit-limited behaviour will occur for a sphere as long as the potential falls off more slowly than r^{-2} everywhere outside the body (Bernstein and Rabinowitz 1959).

For an orbit-limited sphere, the current densities for a Maxwellian distribution are

$$J=J_0(1-q\varphi_s/kT) \qquad \text{for } q\varphi_s<0 \tag{3.2}$$

$$J=J_0\exp(-q\varphi_s/kT) \qquad \text{for } q\varphi_s>0 \tag{3.3}$$

where J_0 is given by

$$J_0=nq(kT/2\pi m)^{1/2}. \tag{3.4}$$

Equation (3.3) holds for any repulsive potential in a Maxwellian plasma as long as the surface is convex and the potential has a monotonic behaviour outward from the surface.

For an orbit-limited cylinder, the current density is

$$J=J_0 2\pi^{-1/2}\,[X^{1/2}+g(X^{1/2})] \tag{3.5}$$

where

$$X=-q\varphi_s/kT>0 \tag{3.6}$$

$$g(s)=\tfrac{1}{2}\pi^{1/2}\exp(s^2)\,\mathrm{erfc}(s). \tag{3.7}$$

Laframboise and Parker (1973) have generalised the concept of orbit-limited motion to include collectors less symmetric than spheres and circular cylinders. They show that a sufficient condition for orbit-limited behaviour is that the curvature of $E=0$ (or $E_\perp=0$) orbits tangent anywhere to equipotentials be always less than that of the equipotentials. Thus prolate and oblate spheroids will have orbit limitation in the Laplace limit as long as the major-to-minor axis ratios are less than 1.653 and 2.537, respectively.

When the current is sheath-limited rather than orbit-limited, the range of integration must be determined from the behaviour of the particle trajectories in the sheath. In general, this is a complicated problem which can only be treated numerically by following particle orbits, and treating the potential distribution self-consistently. Approximate expressions for currents can be obtained by assuming some model distribution for the potential variation in the sheath. Thus Opik (1965) and Parker and Whipple (1967) have obtained the sheath-limited current expressions for power law potentials. Al'pert *et al* (1965) and Whipple *et al* (1974) have obtained currents for the Debye potential. These formulations can be useful in that they give an estimate of the current behaviour as a function of potential for a given Debye length, but it should be recognised that these currents are not obtained from a fully self-consistent treatment.

Laframboise (1966) was the first to develop a general computational procedure for obtaining current–voltage characteristics for spheres and cylinders at rest in a collisionless Maxwellian plasma (see also Parker 1973). Laframboise reviews previous work and presents curves of current plotted against potential for spheres and cylinders for a range of Debye lengths. He also presents charge densities and potential distributions as a function of radial distance in graphical form.

Several workers have derived approximate expressions for the sheath-limited currents to spheres and cylinders based on the idea of a finite sheath surrounding the body (e.g. Allen *et al* 1957, Chen 1965a, b, Lam 1965a, b). It has been shown that the attracted ion current at the sheath edge depends on the electron temperature because of the finite potential drop between the sheath edge and the plasma, the so-called 'Bohm criterion' (Bohm 1949). However, most of this work does not find much application in space for the following reasons: first, in the Earth's upper atmosphere where the plasma density is sufficiently high that the Debye length is small compared to, say, a spacecraft, the equilibrium potential is usually negative and the attracted ion current is dominated by the motion of the body (however, see §4.1). In regions where the body is positive and hence the electron current is sheath-limited, such as the outer magnetosphere or solar wind, then photoemission is a dominant charging current and the space charge in the sheath must take into account the photoelectrons emitted by the body. Formulations of the space charge problem which include the emitted electrons have been made by Chang and Bienkowski (1970), Schroder (1973), Tunaley and Jones (1973), Whipple (1976b) and Parker (1976b). A review of work based on the concept of a finite-thickness sheath may be found in Swift and Schwar (1970).

3.2. Photoemission

The importance of photoemission as a charging process for bodies in space is a result of rather large photoelectric yields for many materials in the extreme ultraviolet range of wavelengths (< 2000 Å) together with significant energy in this same region of the solar spectrum. Figure 1 shows the solar spectrum from 10^2–10^4 Å; the data below 1775 Å are from Hinteregger *et al* (1965) and those above 1775 Å are from Nawrocki and Papa (1961). The Lyman-alpha line at 1216 Å is particularly important; it alone is responsible for as much as 30% of the total photoemitted electrons for some materials. A number of photoelectric yields for tungsten are shown in the same figure: 'dirty' means an untreated surface and 'clean' means the surface was heated at a temperature greater than 1000°C in a vacuum of 10^{-5} Torr until yield reproducibility was established. Hinteregger's data were obtained for an untreated surface; he stated that the yields are reproducible even after exposure to air.

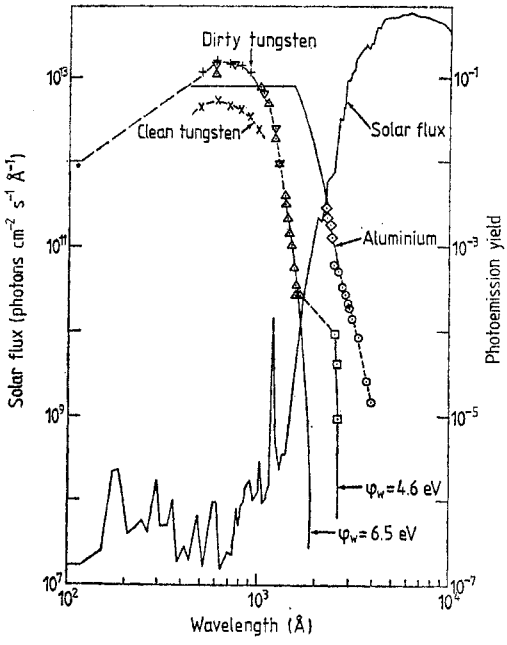

Figure 1. The solar spectrum and photoemission yields. W: △ Hinteregger and Watanabe (1953), ▽ Hinteregger *et al* (1959), × + Walker *et al* (1955), □ Rentschler *et al* (1931), * Lukirskii *et al* (1960). Al: —— Rawer (1963), ◇ Suhrmann and Pietrzyk (1944), ⊙ de Laszlo (1932).

The full curve drawn through Hinteregger's and Watanabe's experimental points to higher wavelengths is a theoretical curve for the yields after Fowler (1931) and DuBridge (1935), with a long-wavelength cut-off at 1900 Å, corresponding to a work function of 6.5 eV. The theoretical curve through the points of Rentschler *et al* (1931) corresponds to a long-wavelength cut-off of 2690 Å (4.6 eV) in good agreement with Warner's (1931) results. The difference in the curves is probably due to the state of the surface, although it is not clear that the Fowler–DuBridge theory can be applied at wavelengths as low as 1700 Å.

When the product of the yield and solar flux is integrated over the spectrum, a total photocurrent of 2.1×10^{-9} A cm^{-2} or 8.1×10^{-9} A cm^{-2} is obtained, depending on which of the two curves is used at the longer wavelengths. These values bracket experimental photoemission current densities from tungsten of 3.9×10^{-9} A cm^{-2} obtained by Hinteregger *et al* (1959) and 5×10^{-9} A cm^{-2} obtained on Explorer 8 (Bourdeau *et al* 1961).

Feuerbacher and Fitton (1972) measured photoemission properties for a number of materials including gold, aluminium, stainless steel, vitreous carbon, graphite and silica, with the surfaces treated so as to simulate space conditions. Graphite was chosen partially because of its possible importance as a constituent of interstellar grains. Figure 2 is taken from their paper, showing the photoelectric yield per incoming photon for some of these materials. The yields are similar to each other for the various materials with a peak yield of the order of 10–25% at 15–20 eV for the photon energy. The yield for graphite is significantly lower, partly because of its higher reflectance. When these yield values were used to obtain the total photoemission current under solar illumination, the results in table 1 were obtained. These currents are in reasonable agreement with measured values in space. For example, Whipple (1965) obtained 3×10^{-9} A cm^{-2} for aluminium. Wrenn and Heikkila (1973) measured photoelectron fluxes above a few eV

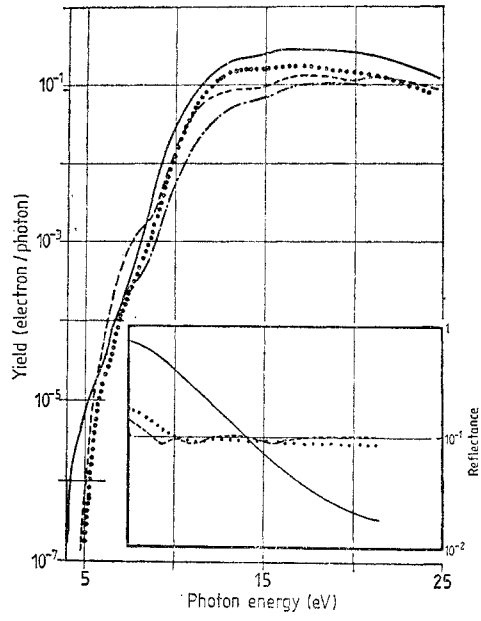

Figure 2. Photoelectric yield per incoming photon for Al (——), Au (– – –), stainless steel (●), and for gold overcoated with 500 Å of carbon (—·—). The reflectance at near-normal incidence for Al, Au and stainless steel is shown in the insert (Feuerbacher and Fitton 1972).

which were consistent with a total current of 5×10^{-9} A cm^{-2} for photoemission from the ISIS 1 and 2 spacecraft surfaces. Norman and Freeman (1973) obtained a value of 8.8×10^{-9} A cm^{-2} for photoemission from a gold surface on OGO 5.

The photoelectric yields in the preceding discussion are for normal incidence of light. Most of the work that has been done in calculating photoemission currents for bodies in space has assumed constant yield per incident photon and used the projected area to correct for the angle of incidence. However, there is evidence that the yield per photon can depend on the angle of incidence. Rumsh *et al* (1960) found a secant dependence for the yields of tungsten, nickel and beryllium in the wavelength range from 1.3–13 Å. Heroux *et al* (1965) found a transition from a secant dependence at 304 Å to nearly angle-independent yields for tungsten at 1216 Å. Samson and Cairns (1965) also found that the angular dependence of the yield for aluminium decreased as the wavelength was changed from 300 to 1300 Å. Juenker *et al* (1965) found a polarisation dependence. When the electric vector was in the plane of incidence, the yield increased roughly as the secant up to about 70°, whereas for perpendicular polarisation it decreased approxi-

Table 1. Integrated photoelectron current under solar irradiation (from Feuerbacher and Fitton 1972).

Material	Photoelectron current (A cm^{-2})
Aluminium	4.8×10^{-9}
Gold	2.9×10^{-9}
Stainless steel	2.4×10^{-9}
Vitreous carbon	2.1×10^{-9}
Graphite	7.2×10^{-10}
Indium oxide	3.2×10^{-9}

mately as the cosine. Katz *et al* (1977) give the following formula for the angular dependence:

$$Y(\theta) = Y(0) \sec\theta \left|\frac{E(\theta)}{E(0)}\right|^2 \left(\frac{1+2d\alpha(0)}{1+2d\alpha(\theta)}\right) \tag{3.8}$$

where $E(\theta)$ is the electric field just inside the solid, $\alpha(\theta)$ is the electric-field attenuation coefficient normal to the surface, and d is the escape depth for photoelectrons.

If the potential distribution around the body in space is such that some of the photoelectrons return instead of escaping, then the angular and energy distribution of the photoelectrons is needed in order to determine the net emission photocurrent. Both laboratory and space experiments indicate that the photoelectrons are emitted isotropically, with a Maxwellian distribution giving a good approximation for the energy spectrum. The characteristic temperature is 1–2 eV (Hinteregger *et al* 1959, Feuerbacher and Fitton 1972, Grard 1973b, Wrenn and Heikkila 1973). The distribution seems to be quite insensitive to the spectrum of the incident light, although strong lines can give some structure to the distribution.

Willis *et al* (1973a, b) have measured the photoelectric yield and electron energy distribution for samples of the lunar surface material. Integration of the yields with a solar spectrum gives a photocurrent of 4.5×10^{-10} A cm^{-2} which is an order of magnitude lower than for typical metals (however, see §9.2). The photoelectron distribution has a weaker tail than a Maxwellian with a characteristic energy of 2.2 eV. Willis *et al* (1973b) have presented data on work functions, photoelectric yields and energy distributions for graphite and vitreous carbon. Draine (1978) has also compiled data on photoemission yields for likely interstellar grain materials. Watson (1973) has suggested that very small spheres with radii comparable to the wavelength of light have their photoemission yields enhanced by a factor of two or more. Thus different size grains in the same environment may come to different equilibrium potentials (Moorwood and Feuerbacher 1976).

3.3. Secondary electron emission by electron impact

When an electron is incident upon a surface, it may be reflected or it may be absorbed into the material. Once it is in the material it may collide with scattering centres and eventually 'back-scatter' out of the material back into space. While the electron is in the material it loses energy and a portion of this energy can go into exciting other electrons which in turn may escape from the material. These three processes of reflection, back-scattering and true secondary emission are usually treated as distinct processes. Reflection is only significant at very low energies, below about 10 eV. Back-scattering refers to electrons which leave the material with a similar but somewhat lower energy than they had upon entering, but with an isotropic distribution due to the randomisation of their velocities. Back-scattering is distinguished experimentally from true secondary emission primarily by the energy of the emitted electrons. Since most secondary electrons are emitted with only a few eV, back-scattering is usually defined only for incident electrons with energy greater than about 50 eV.

The reflection coefficient r is of the order of 0.05 at zero primary energy and decreases with increasing energy according to the relation (Herring and Nichols 1949):

$$r = \frac{W^4}{16(E+W)^3 + W^3} \tag{3.9}$$

where W is the sum of the Fermi energy and work function of the material, and E is the

primary energy, both measured in rydberg units (1 Ryd = 13.54 eV). For example, Guth and Mullin (1941) found r to be 0.05 for tungsten near zero eV. Use of (3.9) with a work function of 3.5 eV and a Fermi energy of 5.6 eV yields a value for r of 0.04 for aluminium. The quantity $(1-r)$ is the sticking coefficient for the material.

Secondary electron emission has turned out to be an important process for spacecraft charging in the magnetosphere. Electron temperatures are frequently in the range of a few hundred eV where the secondary emission yield may be greater than unity. The equilibrium potential of shadowed surfaces is often determined by a balance between incident primary electrons and the resulting secondary emission.

The physical model for the production of secondary electrons involves the excitation of secondaries within the material at a rate proportional to the local energy loss rate by the primaries, the 'stopping power' of the material. The number of secondaries that migrate to the surface and escape decreases exponentially with depth so that only those produced within a thin surface layer contribute significantly to the observed yield. The various treatments of the problem differ primarily in how the stopping power of the material is determined. Reviews of work on secondary emission may be found in Hachenberg and Brauer (1959) and Gibbons (1966).

The shape of the secondary yield curve as a function of primary energy seems to be nearly a universal curve when it is normalised to the maximum yield, δ_m, and the primary energy at the maximum, E_m. Dionne (1973, 1975) has formulated an expression based on a constant stopping power depending only on the primary energy which agrees well with measurements below about $4E_m$. If the angle of incidence of the primaries is also taken into account (Katz *et al* 1977) the expression may be written as follows:

$$\delta = \frac{1.114\delta_m}{\cos\theta}\left(\frac{E_m}{E}\right)^{0.35}\left\{1-\exp\left[-2.28\cos\theta\left(\frac{E}{E_m}\right)^{1.35}\right]\right\}. \tag{3.10}$$

For isotropic primary distributions this expression may be integrated to give an angle-averaged yield:

$$\delta = \frac{2.228\,\delta_m}{Q}\left(\frac{E_m}{E}\right)^{0.35}(Q-1+e^{-Q}) \tag{3.11}$$

where the quantity Q is defined by

$$Q = 2.28\,(E/E_m)^{1.35}. \tag{3.12}$$

The effect of an isotropic flux is to increase the yield and to move the position of the maximum to a higher energy. Table 2 gives some representative values of δ_m and E_m for some typical materials. Dionne (1975) also gives approximate expressions for the crossing energies where the yield parameter crosses unity. These energies play an

Table 2. Representative values for maximum yield, δ_m, and energy at maximum yield, E_m (from Katz *et al* 1977).

Material	δ_m	E_m (keV)
Al	0.97	0.3
Al_2O_3	1.5–1.9	0.35–1.3
MgO	4.0	0.4
SiO_2	2.4	0.4
Teflon	3.0	0.3
Kapton	2.1	0.15
Mg	0.92	0.25

important role in charging balance. For example, in laboratory experiments where a monoenergetic electron beam is incident normally on a surface, the surface tends to take on a potential such that the primaries have the crossing energy when they reach the surface. Katz *et al* (1977) have discussed how experimental stopping power data may be used to obtain more accurate values for secondary emission yields.

The energy distribution for secondary electrons can be approximated by a Maxwellian with a characteristic energy of about 2 eV (Hachenberg and Brauer 1959). Although the literature on secondary emission usually refers to the angular distribution of the emitted secondaries as a 'cosine' distribution, the secondaries are actually emitted isotropically. A small emitting surface emits secondaries into a unit solid angle at the angle θ at a rate proportional to cos θ. This results in an isotropic distribution of secondaries above an extended emitting surface (Whipple and Parker 1969b).

Expressions for the electron back-scattering coefficient have been given by Katz *et al* (1977) based on work by Everhart (1960), Darlington and Cosslett (1972) and McAfee (1976). The angular dependence is given by

$$\eta(\theta)=\eta_0 \cos\theta \tag{3.13}$$

where η_0 is the coefficient for normal incidence. This can be averaged over angles of incidence for isotropic fluxes to obtain an angle-averaged coefficient, or albedo A, given by

$$A=\frac{2}{(\ln \eta_0)^2}(1-\eta_0+\eta_0 \ln \eta_0). \tag{3.14}$$

The coefficient for normal incidence for energies between 10 and 100 keV for materials with atomic number Z can be expressed as

$$\eta_1=1-(2/e)^{0.037Z}. \tag{3.15}$$

Below 10 keV the coefficient should be augmented by an amount

$$\eta_2=0.1 \exp(-E/5000) \tag{3.16}$$

according to data cited by Shimizu (1974). These results have been combined into a formula by Katz *et al* (1977) which takes into account the fact that below 50 eV, back-scattering and secondary emission are indistinguishable:

$$\eta_0=[\ln(E/50)\, H(E-50)\, H(1000-E)/\ln 20+H(E-1000)]\,(\eta_1+\eta_2). \tag{3.17}$$

Here, energies are in eV, and H is the unit step function which vanishes for negative values of the argument. Some typical curves for the coefficient are shown in figure 3.

The angular distribution of the back-scattered electrons may also be taken to be isotropic. The shape of the energy spectrum of the back-scattered electrons may be obtained from the fact that a universal back-scattering kernel based on the relative energies of the incident and back-scattered electrons seems to give a good fit to data. Thus, for an isotropic incident spectrum of monoenergetic electrons, the velocity distribution of the back-scattered electrons is nearly constant up to the velocity of the primaries. The following integral expression may be used to approximate the back-scatter distribution $f(E)$ for an incident, isotropic distribution $f_i(E)$:

$$f(E)=2\int_E^\infty f_i(E')\, A(E')\, \mathrm{d}E'/E' \tag{3.18}$$

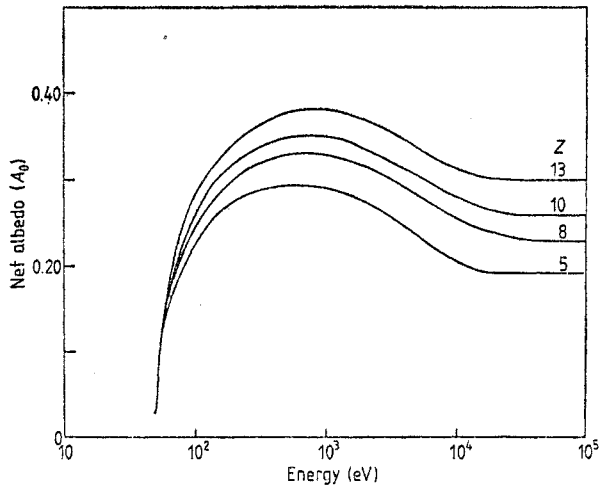

Figure 3. Net albedo plotted against energy for isotropically incident electrons (Katz *et al* 1977).

where $A(E)$ is the albedo as given by (3.14). This is sometimes written in terms of the angle-averaged flux per unit energy, $F(E)=(2\pi E/m^2)f(E)$. Then (3.18) becomes

$$F(E)=2\int_E^\infty F_i(E')\,(E/E'^2)\,A(E')\,dE'. \tag{3.19}$$

This expression has been used not only for back-scattered electrons from solid surfaces (Katz *et al* 1977) but also for electrons coming from the magnetosphere and back-scattering from the top of the Earth's atmosphere (Chiu and Schulz 1978).

3.4. Secondary electron emission by ion impact

The behaviour of surfaces under ion bombardment has been reviewed by Kaminsky (1965), and more recently by McCracken (1975) in this journal. The ions approaching a surface at low kinetic energies (below about 1 keV) are neutralised by Auger emission of an electron where an electron tunnels through the potential barrier to neutralise the ion. The energy released in the process may excite additional electrons which can then be ejected. At higher incident kinetic energies the ions behave similarly to incident electrons in that they can penetrate the surface, scatter, and be re-emitted along with secondary electrons. The fraction that are re-emitted as ions is usually quite small and has been neglected in surface potential calculations. Reflection coefficients for He^+ incident on clean and contaminated tungsten have been measured by Hagstrum (1961) to be 0.0017 and 0.000 43, respectively, and were found to be fairly insentitive to the ion energy. Reflection coefficients for H^+ and O^+ on tungsten or aluminium are probably somewhat larger but still less than 2% (Colligon 1961). At higher energies, the ratio of the charged to total back-scattered particles can be large but the total reflection coefficient is still small.

Figure 4 shows some secondary electron yields for low-energy impact. The number of excited electrons depends on the available potential energy after neutralisation which is determined by the ionisation potential, φ_I, of the incident atom and the work function of the target material, φ_W. When a conduction electron is captured by the incident ion, it makes available a maximum energy of $\varphi_I-\varphi_W$. At least φ_W of this must be used to free another electron from the material so that the condition for secondary emission is

that $\varphi_i > 2\varphi_w$. It is apparent from the figure that the yields for various ions incident on several metals depend primarily on the difference $\varphi_i - 2\varphi_w$.

The curve in figure 4 can be used to estimate the yields for other materials. It should be added that the yield is quite dependent on the condition of the metal surface. Hagstrum's data are for atomically clean surfaces, whereas the platinum in Parker's (1954) measurement may have had some residual impurity.

Knudsen and Harris (1973) have discussed measurements of secondary electrons due to ion impact in space and in laboratory experiments and have found yields approaching 10% for a number of ions, including O^+ and some molecular ions, for incident energies of a few hundred eV. They also inferred that gas contamination of the surface was an important factor in determining yields.

Secondary electron yields due to ion impact can be substantially larger than unity for incident energies above 10 keV. DeForest (1972) showed for a large charging event

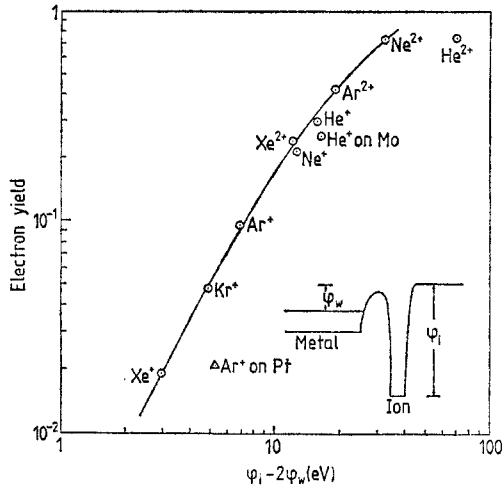

Figure 4. Secondary electron yield for low-energy ion impact. The target is tungsten unless otherwise noted. Circled points are from Hagstrum (1953, 1954) and the triangle from Parker (1954).

on ATS-5 that outgoing secondary electrons were composed almost equally between those due to electron and those due to ion impact. The physical model for the production of secondary electrons upon ion impact is similar to that for electron impact discussed in the last subsection. A simple formula based on a constant energy loss rate by the ions in the material has been shown by Katz *et al* (1977) to fit data for proton impact reasonably well:

$$\gamma = \frac{2\gamma_m (E/E_m)^{1/2}}{1 + E/E_m} \tag{3.20}$$

where γ_m is the maximum yield at an energy E_m. Figure 5 shows this expression fitted to data on proton impact on Al. These yields are for normal incidence. The angular dependence can be taken to be proportional to sec θ. The distribution of the secondaries can be represented well by an isotropic Maxwellian with a temperature of a few eV.

For small bodies such as interstellar grains, the fact that energetic electrons and ions may penetrate completely through the body without being captured may have to be taken into account (Draine and Salpeter 1979).

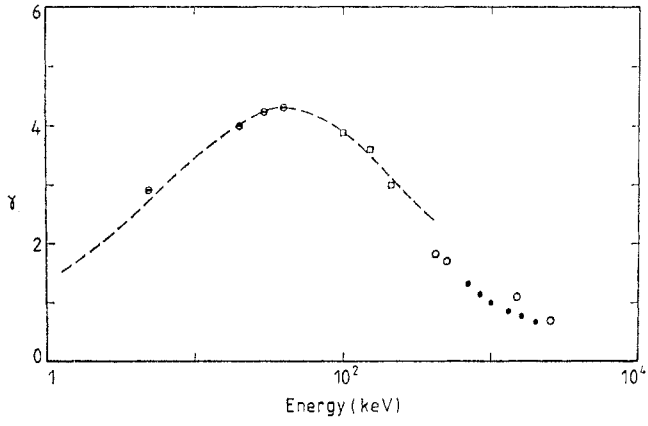

Figure 5. Secondary emission by aluminium for proton impact at normal incidence (Katz *et al* 1977). Broken curve is equation (3.20). ⊖ Cousinie *et al* (1959), □ Hill *et al* (1939), ○ Foti *et al* (1974), ● Aarset *et al* (1954).

3.5. Other charging processes

There are a number of other mechanisms for charge transfer which are significant only in special circumstances. These processes are discussed briefly here; their importance for a particular application must be evaluated individually.

Shen and Chopra (1963) have discussed the effect of *thermionic emission* of electrons from bodies in space. If a work function of 3.5 eV is assumed, which is appropriate for aluminium, a surface temperature of about 800 K is required for an electron emission of 10^5 cm^{-2} s^{-1}. This emission rate is of the order of 1% or less of typical ion fluxes in the solar wind. Such a high temperature is likely only in special situations, such as when a meteor or spacecraft enters the Earth's atmosphere below 100 km at high speeds, or when a body approaches sufficiently close to the Sun. A body with an albedo of 0.4, which is appropriate for meteoroids, will have an equilibrium temperature of 800 K only when it approaches within a distance of 0.19 astronomical units from the Sun—half the distance of Mercury's orbit.

Spitzer and Savedoff (1950) pointed out that for small dust grains *field emission* of electrons will limit the potential when it is negative. The onset of field emission occurs at surface field values between 10^6 and 10^7 V cm^{-1}, the lower field corresponding to an emission flux of 10^5 cm^{-2} s^{-1} for a work function of 3.5 eV. Since the surface field of a small spherical particle is approximately φ/r, the potential φ (in volts) is limited to negative values below approximately $10^6 r$ (r in cm). Thus, field emission is important primarily for dust grains of radii (or surfaces with radii of curvature) of the order of a micron, except when large potentials are expected. Grard (1976) has suggested using field emission to limit negative spacecraft potentials by installation of a probe consisting of many fine wires with sharp tips. Mendis and Axford (1974) give the Fowler–Nordheim formula for field emission flux from a hemispherical surface (of radius r in cm and potential φ in V) in the following form:

$$F=\frac{(\mu/\varphi_w)^{1/2}}{\mu+\varphi_w}\,\varphi^2(60.9-6.8\times10^7\,\varphi_w^{3/2}\,r/\varphi) \tag{3.21}$$

where μ is the Fermi level and φ_w is the work function.

Hill and Mendis (1979) have discussed both field emission and the possible *electrostatic disruption* of bodies by high electric fields (see also Opik 1957, Rhee 1976, Mendis 1979). Disruption will occur if the grain radius is less than a critical value given by

$$r_c = 9.4\, F_t^{-1/2}\, |\varphi| \tag{3.22}$$

where φ is the surface potential in volts, F_t is the tensile strength of the material in dyn cm^{-2}, and r_c is in microns. Figure 6, taken from Hill and Mendis (1979), shows the variation of r_c with $|\varphi|$ for several representative materials. Thus, whereas a grain of

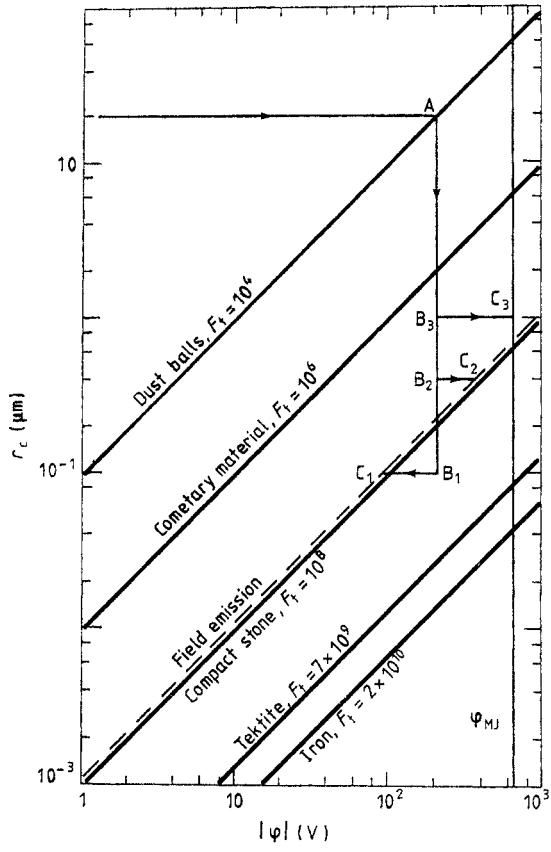

Fignre 6. Critical radii for grains of different material and varying potentials against electrostatic disruption (Hill and Mendis 1979). Stable regions are above the diagonal lines. Lines with arrows indicate possible paths of fragments. The field emission limit is also shown.

iron charged to a potential of -800 V is stable against disruption if its radius is greater than 0.06 μm, a loose dust ball charged to the same potential would be stable only if its radius was greater than 80 μm. The figure also shows the potential limitation due to field emission (broken curve), based on a critical surface field of 10^7 V cm^{-1}.

Radioactivity in a body in space constitutes a charging mechanism both through the escape of emitted charged primaries from the radioactive nuclei and also through the escape of secondary electrons excited by the primary in its passage to the surface. Whipple (1965) has shown that the amount of ordinary radioactive material in bodies is insignificant for charging effects. Yanagita (1977) has suggested that grains formed in novae or

supernovae may have significant radioactive levels, particularly ^{22}Ni or ^{26}Al which are beta emitters. The charging due to beta emission would vary as the volume of the grain, and hence larger grains would tend to be positive. Satellites sometimes carry quantities of radioactive materials in conjunction with certain types of experiments, or as a power source. Such sources are usually well shielded but may constitute possible charging mechanisms.

Impact ionisation occurs when a neutral atom or ion strikes a surface with sufficient kinetic energy that either the incident neutral or atoms on the surface are ionised with subsequent escape of ions and/or electrons. This phenomenon has been observed on the Pioneer Venus Orbiter (Brace 1981) on a Langmuir probe which detected extra electrons correlating with the neutral atmospheric density. The effect was largest at periapsis where the neutral density was largest and where the spacecraft velocity was such that the incident CO_2 had a kinetic energy of about 20 eV. This effect has also been seen by the Atmospheric Explorer C satellite in Earth orbit (Hanson *et al* 1981) where the ions were identified as coming from the spacecraft because of their low energy. The ion fluxes decreased gradually with time, indicating a cleaning up of the spacecraft surface.

A phenomenon similar to impact ionisation is *impact vaporisation* (also sometimes called impact ionisation) where a small particle such as a dust grain vaporises and ionises into a cloud of plasma upon impacting a surface at high speed. The charged particles in the cloud can either escape or be collected depending on the electric-field configuration. This has been suggested as an important charging mechanism for a space probe entering a cometary atmosphere (Grun 1980). The mechanism has also been investigated for the purpose of developing detectors for micrometeoroids (McDonnell 1978, Fechtig *et al* 1978).

Enhanced ionisation of neutral gas in the vicinity of a body in space can occur at times and lead to charging currents. The ionisation of outgassing material from a spacecraft and subsequent return of the ions to a negatively charged spacecraft has been discussed by Cauffman (1980) and observed on the ATS-6 and SCATHA spacecraft. The ions can be easily identified since they arrive at energies less than the spacecraft potential. Enhanced ionisation of either outgassing material or the environmental neutral gas by returning primary and/or secondary electrons or by a beam–plasma interaction is probably the source of the large return currents observed in some experiments where energetic electron beams were emitted from vehicles in the ionosphere (e.g. Winckler 1980). This phenomenon will be discussed further in §8.

Finally, there can be *enhanced collection of electrons* due to radio-frequency fields (Takayama *et al* 1960). There is a rectifying effect on the plasma electrons when the radio frequency is near or below the local plasma frequency. At low frequencies the additional current density is obtained by integrating equation (3.3) over one period of the wave:

$$J = J_0 I_0(eV/kT) \tag{3.23}$$

where J_0 is given by (3.4), I_0 is the modified Bessel function of the first kind, V is the amplitude of the RF voltage and T is the electron temperature. The current is independent of frequency until close to the plasma frequency (f_p) where it rises to a maximum and then falls to zero at higher frequencies. The shape of the maximum depends on geometry and on the nature of damping effects in the plasma which can be either collisional or due to phase mixing (Harp and Crawford 1964, Crawford and Harp 1965). Whale (1964) showed that for a cylindrical dipole antenna the peak of the resonance occurs at $f_p/2^{1/2}$. The current at the peak of the resonance can be enhanced by as much as several factors of 10 at ionospheric electron densities.

4. Effects of non-isotropic plasmas and magnetic and electric fields

4.1. Currents to a moving body

When the undisturbed plasma is not isotropic, information about the particle trajectories is required in order to evaluate the distribution function at the surface of a body. In general, this requires a calculation of particle orbits unless there is some kind of symmetry involved so that angular momentum conservation can be used. The most important anisotropy for surface potential calculations is that due to motion of a body through the plasma. In the reference frame of the body, the plasma appears to have a net streaming velocity. Thus in the ionosphere where a typical satellite velocity is about 8 km s^{-1}, the ions will appear to have their velocity distribution shifted by this amount since the satellite speed is large compared to typical ion thermal speeds. On the other hand, the electrons will still appear to be isotropic since their thermal speeds are much larger than the satellite speed.

In this section we give some formulae which may be used to estimate the ion current to a moving body in a plasma under certain circumstances. The general problem of the current to a moving body for arbitrary Debye lengths has not been treated exactly, so it is difficult to assess the accuracy of the approximations. We consider the total current to a body which implies that the body has a conducting surface at a given potential. For an insulating surface, the current density as a function of position would be needed; in such a case, the surface would not be an equipotential and hence the electric field near the surface would need to be known to obtain the currents.

In addition to the motion of a body through the plasma, there can be net drifts of the plasma due to convection electric fields. In the magnetosphere the plasma is frequently pitch-angle-dependent, especially for directions closely aligned with the magnetic field. Vogl *et al* (1976) have pointed out that fluxes of field-aligned electrons can at times dominate the charging in cavities on spacecraft even though the anisotropic component is small compared to the total flux.

In the case of a moving body, numerical work indicates that the potential distribution in front of spheres and in front of cylinders moving perpendicular to their axes has approximately the same symmetry as the body (Al'pert *et al* 1963, Fournier 1971). Since most of the ion current is collected on the front surface of the body, this symmetry can be used to obtain expressions for the current. Hinteregger (1961) and Kanal (1962) derived the following formula for the current to a moving sphere with radius R at a repulsive potential ($q\varphi > 0$):

$$I=\frac{\pi R^2}{2} nqV\left(\left(1+\frac{\alpha^2}{2V^2}-\frac{U^2}{V^2}\right)\left[\operatorname{erf}\left(\frac{V+U}{\alpha}\right)+\operatorname{erf}\left(\frac{V-U}{\alpha}\right)\right]\right.$$
$$\left.+\frac{\alpha}{\pi^{1/2}V}\left\{\left(\frac{U}{V}+1\right)\exp\left[-\left(\frac{V-U}{\alpha}\right)^2\right]-\left(\frac{U}{V}-1\right)\exp\left[-\left(\frac{V+U}{\alpha}\right)^2\right]\right\}\right) \tag{4.1}$$

where V is the velocity, $U=(2q\varphi/m)^{1/2}$ and α is the thermal velocity of the ions, $\frac{1}{2}m\alpha^2=kT$. In the limit of large V/α, this expression reduces to

$$I=\pi R^2 nqV\left(1-\frac{2q\varphi}{mV^2}\right) \tag{4.2}$$

which gives a linearly decreasing current as the potential is increased. The current expression in (4.1) is independent of sheath size or variation of potential through the sheath as long as the electric field is radial. Gringauz and Zelikman (1957) showed that this is

because the current is limited by angular momentum considerations, and is true as long as the effective radius, given by

$$R_{\text{eff}} = R\left(1 - \frac{2q\varphi}{mV^2}\right)^{1/2} \tag{4.3}$$

is less than the 'sheath' radius. This is always true for repulsive potentials since the quantity in the parentheses of (4.3) is always less than unity. In addition, it will be true for attractive potentials until the effective radius exceeds the sheath radius, so that (4.2) may also be used for a limited range of attractive potentials.

An analytic expression for the general case of the ion current to a moving body in an attractive field is not yet available. When the body is small compared to a Debye length so that the field may be assumed to be a Coulomb field, the current for an attractive potential has been derived by Kanal (1962):

$$I = \pi R^2 nqV\left[\left(1 + \frac{\alpha^2}{2V^2} + \frac{U^2}{V^2}\right)\operatorname{erf}\left(\frac{V}{\alpha}\right) + \frac{\alpha}{\pi^{1/2}V}\exp\left[-(V/\alpha)^2\right]\right]. \tag{4.4}$$

In the other limit when the Debye length is very small, expression (4.4) with the potential set equal to zero may be used either with the cross section of the body (πR^2) or with the cross section of the body plus sheath (πa^2) where $a = R + t$. Expressions for the sheath thickness t which have been suggested are

$$t = 0.83\, L(R/L)^{1/3}(q\varphi/kT)^{1/2} \tag{4.5}$$

(Walker 1964) or

$$t = 0.93\, L(8q\varphi/\pi mV^2)^{3/4} \tag{4.6}$$

(Parks and Katz 1981). The latter is based on the theory of the sheath around a spherical body at a high potential given by Langmuir and Blodgett (1923, 1924) and Al'pert *et al* (1965). Parker (1980) has also given analytic expressions for the sheath radius based on the Langmuir and Blodgett (1924) work. However, all of these expressions for sheath size were derived for a stationary plasma and it is not known how well their use in this way approximates the actual current in a moving plasma.

A number of workers have made numerical calculations of the ion current to an attractive moving sphere or cylinder. Kanal (1962) and Walker (1964) both made simplifying assumptions about the structure of the sheath in order to obtain currents. Whipple (1965) used expression (1.1) without linearisation for the space charge and obtained currents numerically as shown in figure 7. At low potentials the currents follow (4.2) but at higher potentials the currents show saturation as the sheath size limits the current. Parker and Whipple (1970) used trajectory calculations to obtain the current density as a function of angle with respect to the direction of motion in a potential distribution resulting from a linearised space charge expression. Whipple *et al* (1974) obtained an integral expression for the current density to a moving sphere with a Debye potential. Godard (1975) used the self-consistent potential profiles of Laframboise (1966) for a stationary body to calculate currents due to a drifting plasma; the range of parameters for which his results are valid was tested in laboratory experiments by Makita and Kuriki (1978).

Fournier (1971) obtained the current self-consistently for a cylinder in a flowing plasma. Parker (1973) described a systematic procedure for obtaining a self-consistent solution for the current and potential distribution in front of a sphere, assuming spherical symmetry.

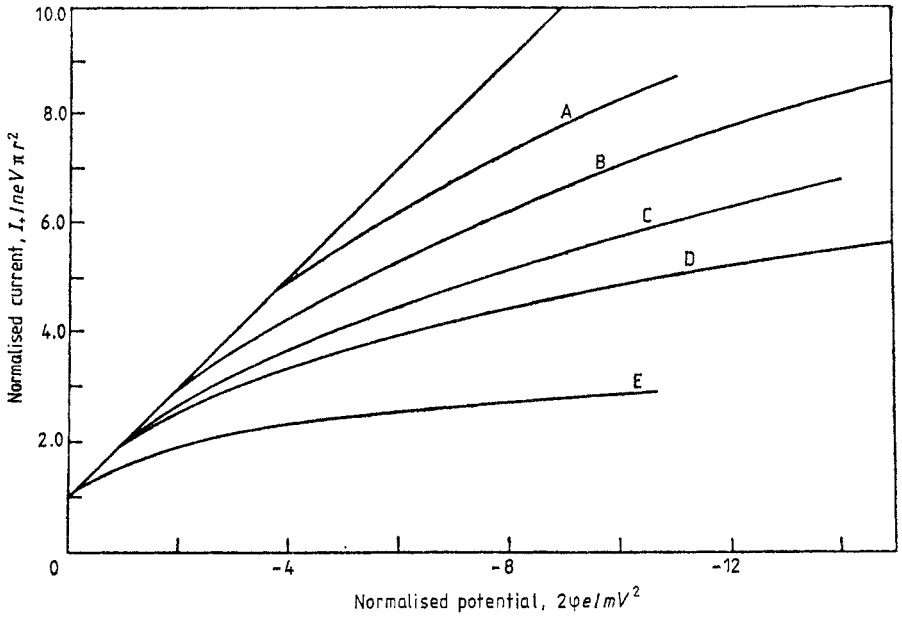

Figure 7. Ion current to a large, moving negative sphere. A, $r/L=10$, $1/2mV^2=50\,kT$; B, $r/L=10$, $1/2mV^2=33\,kT$; C, $r/L=10$, $1/2mV^2=20\,kT$; D, $r/L=5$, $1/2mV^2=2\,kT$; E, $r/L=10$, $1/2mV^2=2\,kT$.

4.2. Wake effects

The plasma wake behind a moving body is a cone-shaped region depleted unequally of both ions and electrons because of the small thermal velocities of the ions compared to the streaming velocity. Electrons can readily penetrate this region until the negative space charge from the excess electrons builds up the negative potential to a value such that they also are depleted. There can be flaring and periodic structure in the far wake. The potential distribution in the wake does not appreciably affect the total ion current to the body because most of the ion current is incident on the front. However, the electron current to the back surface will be reduced because of the negative potential barrier in the wake. Measurements of electron current on Explorer 8 (Bourdeau and Donley 1964) found a reduction of about 15–30% on the back with respect to the current in front, whereas on both Ariel 1 (Samir and Willmore 1965, Henderson and Samir 1967) and Explorer 31 (Samir and Wrenn 1969) the reduction was as much as two orders of magnitude. This was explained by Samir (1970) who showed that the difference was due to the ion composition. For the data of Explorer 8 the dominant ion was He^+ whereas the large reductions for the Ariel 1 and Explorer 31 data were for a dominant ion of O^+. Figure 8 from Samir (1970, also Samir 1973) shows how the reduction in electron current on the downstream side of Explorer 31 varied with the average ion mass.

Figure 9 from Samir and Wrenn (1969) shows how the electron current density varies as a function of the angle of attack. Gurevich *et al* (1969) give a complicated analytic expression for the current density as a function of angle. However, to zero order for $90° < \theta < 180°$, the current density varies as

$$\ln\left(J(\theta)/J_f\right) = -\cos\theta \ln \delta_m \tag{4.7}$$

where δ_m is the ratio of the back-to-front current and J_f is the current density on the front.

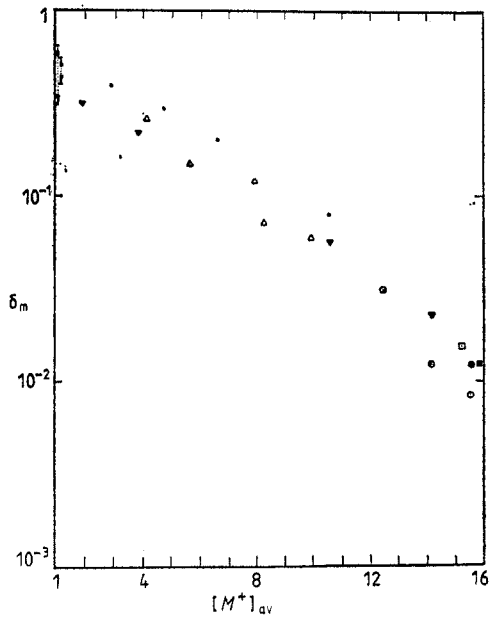

Figure 8. Variation of the back-to-front current ratio, δ_m, with the mean ion mass (after Samir 1970, 1973). ●, pass number 346, △ pass number 393, ■ pass number 683, ⊙ pass number 695, ⊡ ⊗ pass number 706, ▼ pass number 727.

This expression can be integrated over the rear surface of a sphere to obtain

$$I_{\text{back}} = 2\pi R^2 J_f \left(\frac{1-\delta_m}{-\ln \delta_m} \right). \tag{4.8}$$

The quantity δ_m can be obtained from the following expression according to the data of Samir (1970):

$$\delta_m = \exp(\varphi_w e/kT) \tag{4.9}$$

where

$$\frac{\varphi_w e}{kT} \simeq -0.7 - 0.19 \left(\frac{\bar{m} V^2}{2kT} \right). \tag{4.10}$$

Here, φ_w can be regarded as the effective value of the potential barrier in the wake with respect to the satellite; $\bar{m}$ is the mean ion mass and V is the spacecraft velocity. The quantity in parentheses in (4.10) is the square of the ion Mach number. The potential in the wake should also depend on the Debye length; Al'pert *et al* (1963) give a value of $-(2kT/e) \ln (R/L)$ for the largest (negative) potential in the wake, and Samir *et al* (1979, 1980) have shown that the ion depletion in the wake does indeed depend on the Debye length to body ratio. However, the dependence of electron current on Debye length has not yet been experimentally verified. Apparent enhancements of the electron temperature in the wake (Samir and Wrenn 1972, Oran *et al* 1975) are probably due to the angular-dependent potential barrier in the wake preventing some of the electrons from reaching the electron probe and thus causing a distorted current–voltage characteristic (Illiano and Storey 1974, Troy *et al* 1975). However, there may also be heating by wave–particle interactions. Comparisons of experimental data on wake structure with various theoretical models have been made by Samir and Jew (1972) and Samir *et al* (1975). Labor-

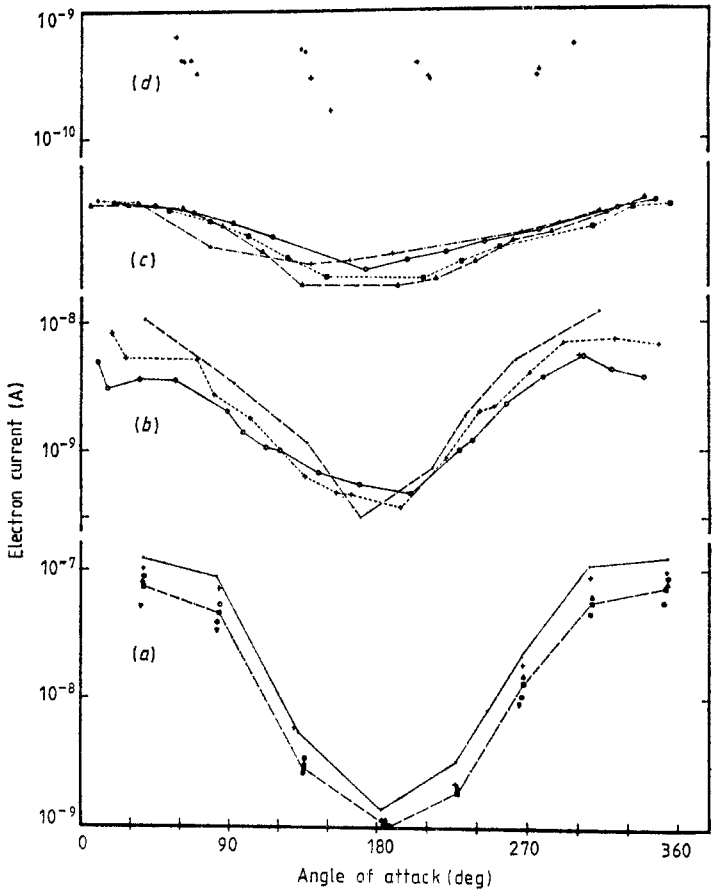

Figure 9. Measured electron current plotted against angle of attack (Samir and Wrenn 1969), from a Langmuir probe on the Explorer 31 satellite. (*a*) Day 15, 1966; pass 565; LT range: 15 h 50 m–16 h 30 m; magnetic latitude range: −17––43; magnetic longitude range: −4–2. Altitude: ● 660–631, + 27–601, ⊙ 598–579, ▲ 576–561, ■ 556–543, ● 541–535, ▼ 532. (*b*) Day 352, 1965; pass 225; LT range: 06 h 34 m–07 h 00 m; magnetic latitude range: −36––8; magnetic longitude range: 85–94. Altitude: ● 620–720, +720–820, ⊙ 820–910. (*c*) Day 355, 1965; pass 267; LT range: 18 h 48 m–19 h 11 m; magnetic latitude range: −12––38; magnetic longitude range: 85–82.5. Altitude: ● 1685–1585, + 1585–1485, ⊙ 1485–1385, ■ 1385–1285, ▲ 1285–1175. (*d*) Day 350, 1965; pass 204; LT range: 08 h–08 h 40 m; magnetic latitude range: 56–64; magnetic longitude range: 69–80.5. Altitude: +2060–2280.

atory studies of wake structure have been carried out by Hester and Sonin (1970), Fournier and Pigache (1975) and Stone *et al* (1978).

The effect of the plasma wake could be especially important for a body with an insulating surface. Parker (1978) and Chang *et al* (1979) have shown that the downstream surface of such a body could charge to a potential corresponding to the streaming energy of the ions. Mendis *et al* (1981) have applied this argument to comets in the distant solar wind to obtain potentials as large as −2500 V on the dark side.

4.3. Magnetic and electric fields

There has been a great deal of work on the effect of a magnetic field on the collection of particles by a probe in a laboratory plasma. The finite length of the field line results in

depletion of the plasma on the magnetic tube intersecting the probe. Consequently the current is strongly limited and depends critically on the kind of cross-field transport mechanism that is available (e.g. Bohm *et al* 1949, Simon 1955, Bertotti 1961, Sanmartin 1970). In space, the field lines are essentially infinite in length compared to the dimensions of a body such as a spacecraft. In addition, there is usually enough relative motion due either to the body motion or to plasma drifts that depletion of any particular flux tube extends only over a small distance. Laframboise and Rubinstein (1976) treated collection by a cylinder, and Parker and Murphy (1967) treated electron collection by a positively charged sphere in a magnetoplasma where the current was limited by cross-field drift motion. Parker and Murphy show that the current is a function of the quantity (φ/R^2B^2) and obtain numerical results for potentials below a critical potential which is 3400 V for a 1.5 m sphere in the ionsophere ($B=0.45$ G). At higher potentials only an upper limit for the current was obtained which varies as $(\varphi/R^2B^2)^{1/2}$. The same dependence was obtained by Rubinstein and Laframboise (1978) for an infinite cylinder. However, Linson (1969) has argued that turbulent diffusion across field lines will increase the current considerably above these values, except when the background electron concentration is low. When the parameter $q=\omega_p{}^2/\omega_c{}^2$, where ω_p is the plasma frequency and ω_c is the gyrofrequency, exceeds a critical value of the order of unity but which is perhaps as low as 0.05, the plasma is unstable to the growth of turbulence.

At low potentials or when the Debye length is small compared to body size so that the body dimensions can be used for the collecting area, it may be important to consider magnetic shadowing effects. For example, the effective collecting area of a sphere changes from the full surface area for gyroradii large compared to the sphere radius to twice the cross section of the sphere for small gyroradii. Figure 10 from Whipple (1965) shows how the current varies to a sphere as a function of the most probable gyroradius in a Maxwellian plasma. The effect of magnetic shadowing on or above the lunar surface has been discussed by Reiff (1976) for an isotropic plasma and by McGuire (1972) for a drifting plasma.

The most significant large-scale electric field that a body in space experiences is the

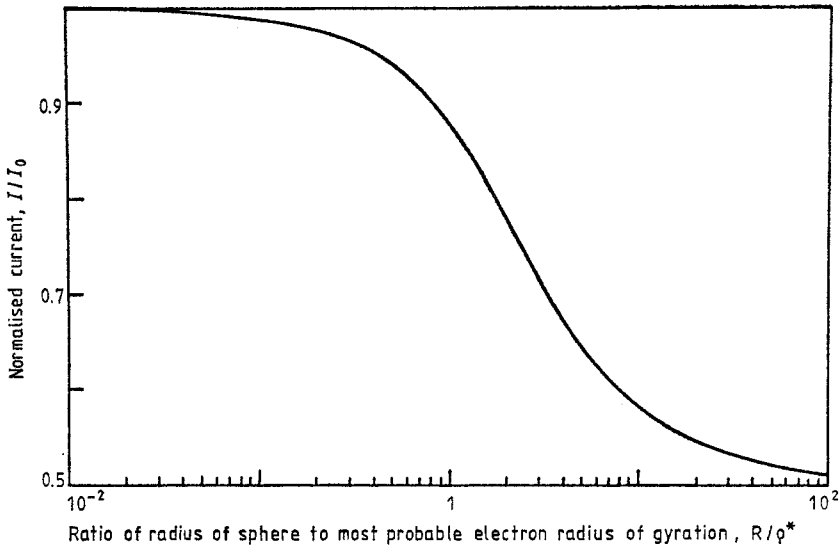

Figure 10. Electron current to an uncharged sphere in a magnetic field.

induced field due to the motion of the body across magnetic-field lines. In the reference frame of the moving body this is a real electric field which is superimposed upon any other electric fields that are present. This means that the potential of the body does not have a unique reference in the plasma, but rather the potential difference between even a conducting body and the plasma varies with position on the body because of the potential gradient in the plasma. Most treatments of the effect of the induced electric field on current collection have taken the usual current expressions for a probe in a plasma and substituted the local potential drop as a function of position to obtain a net current. Thus Beard and Johnson (1960) found the current to a parallelepiped, and Whipple (1965) obtained the following expression for the electron current to a sphere of radius r:

$$I = I_0 \frac{\sinh (e|\boldsymbol{V}\times\boldsymbol{B}|\, r/kT)}{e|\boldsymbol{V}\times\boldsymbol{B}|\, r/kT} \tag{4.11}$$

where the potential of the sphere is everywhere negative with respect to the plasma and I_0 is the electron current that would be collected if there were no induced field. However, it is not clear that the orbit-limited equations can be applied in this situation since the potential does not decrease monotonically outwards in all directions.

An important consequence of the induction effect is that large bodies can have large potential differences with respect to the plasma. One end of the body can be pinned close to zero volts, or slightly positive, with the other end becoming relatively more negative. Morrison *et al* (1978) have discussed the current collection by a long wire in near-Earth orbit and have shown that kilovolt potential differences can develop between one end of a 10 km wire and the adjacent plasma (see also Williamson and Banks 1976). This effect may also be the driving mechanism responsible for the acceleration of particles in the vicinity of Jupiter's satellite Io (see §9.3).

5. Calculation of surface potentials

5.1. Equilibrium potential and charging times

The problem of calculating the equilibrium potential of a body in a given environment involves determining the important charging currents to the body as a function of potential and finding the potential at which the total current vanishes. Even in the simple case of a small stationary sphere in a Maxwellian plasma such that the only charging currents are those given by (3.2) and (3.3), the resulting equation for the equilibrium potential is a transcendental equation which must be solved numerically. Thus in a hydrogen plasma, the equilibrium potential in such a case is $(\varphi e/kT) = -2.5$ for equal ion and electron temperatures.

When a body has non-conducting surfaces or several isolated conducting surfaces then the current balance has to be performed locally or for each surface separately. The effects of such differential charging of surfaces are discussed in §6.

Figure 11 shows schematically two current–voltage curves for a hypothetical body. The equilibrium potentials where the curves cross the zero-current level are also shown. Usually the current–voltage characteristic of a body is 'normal' in that it is monotonic and crosses the zero-current level only once. The equilibrium potential for such a body is stable: for a slight perturbation of the charge on the body, the system will move in the direction shown by the arrows and hence tend to restore the system to its equilibrium value. However, it is possible to have abnormal behaviour of current–voltage curves, as shown by the characteristic with three equilibrium potentials. Here, φ_1 and φ_3 are

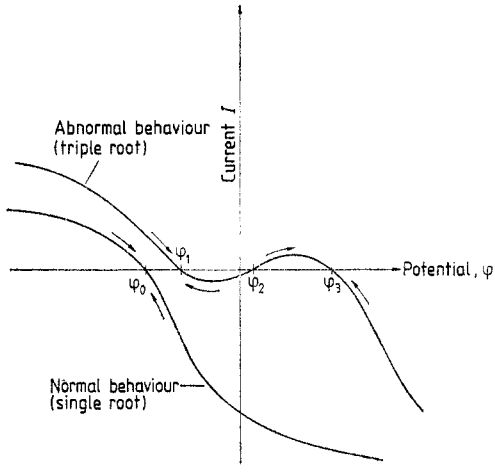

Figure 11. Two current–voltage curves for a hypothetical body illustrating stable and unstable equilibrium potentials.

stable, but the centre potential φ_2 is unstable in that the system will tend to move away from this value if there is a perturbation. Sanders and Inouye (1978) and Prokopenko and Laframboise (1977, 1980) have shown that such abnormal curves are possible for materials in the Earth's magnetosphere because of the shape of secondary electron emission currents plotted against body potential when the environmental plasma is not Maxwellian. These authors point out that it might be possible to have sudden changes in the body potential when the environment is changing slowly if the current–voltage curve evolves from a multiple-root to a single-root configuration.

The concept of equilibrium potential is useful because the charging time for a body is usually, but not always, small compared to the time for changes in the environment. The charging time τ can be estimated from figure 11: $\mathrm{d}Q/\mathrm{d}t=(\mathrm{d}I/\mathrm{d}\varphi)_{\varphi_0}\Delta\varphi$ and hence $\tau=RC$, where C is the capacitance of the body (e.g. equation (1.5)), and R is a 'resistance' given by $R=|(\mathrm{d}I/\mathrm{d}\varphi)_{\varphi_0}|^{-1}$. A useful estimate for R is that $R\cong(kT/e)\,(JA)^{-1}$, where the current density J and temperature T refer to the current constituent which is most rapidly changing at φ_0. For a body small compared to a Debye length, the charging time increases inversely with the radius because of the presence of the area A in the denominator of the resistance. Time constants for spacecraft are of the order of ms in the magnetosphere, but can be much longer for dielectric surfaces with large capacitances to substrate material. Thus a spinning spacecraft with exposed insulating surfaces may never reach equilibrium. Charging times for 10 μm dust grains are of the order of ms in the ionosphere but of the order of tens of minutes in interplanetary space. Hill and Mendis (1979) have had to follow the time-dependent charging of dust grains moving through the Jovian magnetosphere because the charging currents varied on a time scale comparable to the charging time of a few hours. Otherwise, equilibrium potentials have been assumed in charging calculations except in cases where differential charging was an important factor.

5.2. Calculated potentials for various environments

In this subsection we give some typical results of equilibrium potential calculations for bodies in various environments, starting in the Earth's ionosphere and moving outwards.

The results may be summarised as follows: in the ionosphere, potentials are of the order of a few tenths of a volt negative, corresponding to a few (kT/e), due to a balance between the collection of plasma electrons and ions swept up by the body's orbital motion. At higher altitudes, photoemission becomes important and positive potentials start to occur at altitudes where the plasma density falls below about 10^3 cm^{-3}. In the magnetosphere, potentials are usually a few volts positive except in disturbed conditions where they may become highly negative, especially in eclipse, because of high electron temperatures and the disappearance of cold plasma. In the solar wind, potentials are again usually a few volts positive. Potentials in the magnetospheres of other planets are similar to those in the Earth's except that photoemission becomes less important for planets more distant from the Sun. In interstellar space, the potentials depend strongly on the radiation field and on the local plasma properties and can be a few volts positive or negative.

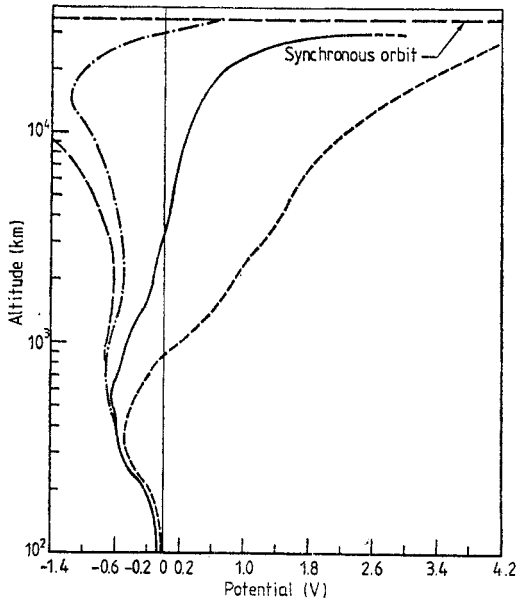

Figure 12. Satellite potentials as a function of altitude of circular orbit (Kasha 1969) for four values of photoemission current. The full curve is for a photoemission current of 3×10^{-9} A cm^{-2}. ———, $i_{ph}=0$; —·—, $i_{ph}/ne \times 0.1$; --- $i_{ph}/ne \times 10$.

Figure 12 is taken from Kasha (1969) showing potentials for a hypothetical 1 m diameter metal satellite at altitudes from 100 km to synchronous orbit. The four curves are for four values of photoemission current; Kasha includes attraction effects on both ions and electrons where appropriate but without any shielding effects of the plasma. The satellite velocity is assumed to be that appropriate for a circular orbit at that altitude. The effects of the wake and of the magnetic field in restricting electron fluxes are included approximately. A plasma profile was used where the electron temperature increases to 2 eV at the highest altitude and where the density exhibited a 'knee' characteristic of the plasmapause at about 20 000 km altitude.

The positive potentials that Kasha obtained at the higher altitudes were limited to about +4 V because he used a photoelectron temperature of 1 eV. Shkarofsky (1971)

used a similar formulation for the currents to a satellite between 150 and 4000 km but with photoelectron temperatures of both 1 and 3 eV. He found that positive potentials of +4.9 V might occur for the higher photoelectron temperature at 4000 km altitude in the polar trough of the ionosphere where the electron density can be below 100 cm^{-3}. The overall variation covering minimum and maximum conditions was between −1.0 and 2.1 V for the lower (1 eV) and −1.0 and +4.9 V for the higher (3 eV) photoelectron temperature. Neither of these authors included effects due to energetic particles or secondary electrons.

Kurt and Moroz (1962) seem to be the first to point out that large energetic particle fluxes in the magnetosphere could lead to large (i.e. kilovolt) negative potentials on spacecraft. They included secondary electron emission effects from both incident ions and electrons as well as photoemission and plasma currents. At that time the energetic particle fluxes and plasma properties in the magnetosphere were not well known. Whipple (1965) also mentioned the possibility of large negative potentials. Knott (1972) calculated equilibrium potentials in anticipation of the ISEE spacecraft using measured spectra for the plasma and energetic populations outside the plasmasphere and secondary emission properties for various materials. He found that large negative potentials of up to about −3 kV could develop in eclipse situations. He also pointed out that materials with high secondary electron yields could be used to avoid highly negative charges. When DeForest (1972) measured potentials up to −10 kV on ATS-5 in eclipse and several hundred volts negative in sunlight, he was able to explain the charging with a mathematical model which required secondaries from both electron and ion impact as well as photoemission and the plasma currents. Fairly simple current balance models based on Maxwellian or biMaxwellian plasmas and typical material properties for photoemission and secondary yields have proven to be quite effective in qualitatively explaining observed potentials in the magnetosphere (e.g. Garrett 1979). A quantitative comparison between calculated and observed potentials requires detailed information on both spacecraft configuration and material properties and on the environmental plasma characteristics.

In the solar wind the predominant charging mechanisms are photoemission and collection of plasma electrons. The solar-wind ion flux contribution is of the order of two orders of magnitude smaller than the photoemission current. Typical equilibrium potentials are a few volts positive (e.g. Rhee 1967, Wyatt 1969). The potential is fairly independent of distance from the Sun since both the electron density and the photoemission current vary inversely with the square of the distance from the Sun (Parthasarathy 1978). Thus spacecraft, dust grains and the front sides of objects like the Moon which are exposed to the solar wind all have similar equilibrium potentials. However, surfaces which are shielded from sunlight and from solar-wind ions such as the dark sides of the Moon, asteroids or comets may attain large negative potentials as was mentioned in §4.2 (e.g. Knott 1973, Parker 1978). Solar-wind electrons can still reach these surfaces, but the equilibrium potential will depend critically on the mechanism for positive currents. Mechanisms which have been discussed for the Moon are secondary electrons coming from the surface, and ions coming from ionisation of the lunar atmosphere and subsequent acceleration to the surface (Manka 1972, Manka and Michel 1973, Lindeman *et al* 1973).

The potentials of spacecraft near other planets have been discussed by a few authors. Robinson and Holman (1977) modelled the charging of the Pioneer Venus Orbiter and calculated potentials of less than a volt. However, very large negative potentials may occur on spacecraft in the magnetospheres of Jupiter and Saturn. Scarf (1975) pointed out that if the cold plasma had low densities, potentials could perhaps reach hundreds

of kV. Goldstein and Divine (1977) and Sanders and Inouye (1978) also predicted potentials as large as tens of kV near Jupiter, especially for shadowed surfaces.

The problem of grain potentials in interstellar space was the initial impetus for work on charging (see §2.1). Most of the work on charging in astrophysical regimes other than the solar system has focused on interstellar grains. Summaries of earlier work are contained in papers by Aannestad and Purcell (1973), Wesson (1974) and Mendis (1979). Almost all the predictions are of potentials of a few volts, with the polarity depending on the relative contributions of particle collection from the interstellar plasma as against photoemission and, in some regimes, secondary electron emission. Feuerbacher *et al* (1973) balanced photoemission against ion and electron collection, using different radiation fields with two different grain materials for calculating the photoemission current. In H I regions they used a diluted 10^4 K black-body spectrum and a spectrum derived by Habing (1968) which was rather flat between 912 and 2400 Å. They give plots of the equilibrium potential against the ambient electron density with different plasma temperatures as a parameter. The potentials are positive at low plasma densities, with the low-yield material (graphite) going through zero at about 10^{-2} cm^{-3} for the spectrum of Habing and at about 10^{-3} cm^{-3} for the black-body spectrum. Potentials for the higher yield material (aluminium oxide) go through zero at electron densities about an order of magnitude larger. Figure 13 shows their results for an H II region using a B0 star for the source of the radiation field. The potentials are given as a function of electron density or as a function of distance from the exciting star for an electron density of 10 cm^{-3}.

Hayakawa (1976) suggested that high-speed grains expelled from cool stars might go to +40 V because of secondary electron emission by ion impact. Burke and Silk (1974) and Draine and Salpeter (1979) calculated potentials for grains in hot interstellar gas taking into account the additional processes of secondary emission, field emission and

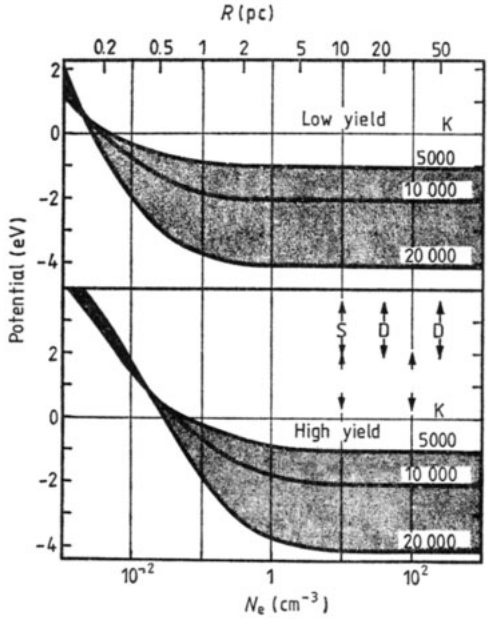

Figure 13. Equilibrium potential of interstellar grains in an H II region at 10 pc from the exciting B0 star (Feuerbacher *et al* 1973). The scale at the top shows the potential as a function of the distance from the exciting star for a constant electron density of 10 cm^{-3}.

penetration of fast particles through the grains. They found that positive potentials are likely in hot gases because of secondary emission. Gail and Sedlmayr (1975) and also Simons (1976a, b) discussed the statistics of charges on grains due to the discreteness of the elementary charge. For small grains where the equilibrium potential corresponds to only a few elementary charges, there will be a distribution of charges centred at the equilibrium charge for otherwise identical grains. For very small grains the image force of charged particles near a grain may have to be taken into account in the charging process (De 1974, Simpson *et al* 1978).

6. Differential charging, potential barriers and discharge processes

6.1. Effects of differential potentials

Early work on differential potentials on spacecraft surfaces was prompted by concerns over effects of such potentials on spacecraft experiments. Whipple and Parker (1969a, b) showed that drawing-in potentials used on aperture grids and guard electrodes of electron-trap experiments could attract photoelectrons and secondary electrons into the collectors even when the spacecraft itself was at a negative potential. The potential distribution in the vicinity of the aperture formed a potential barrier that prevented such secondary electrons from escaping from the spacecraft. Anomalously high electron densities that had been inferred from experiments in the solar wind, and more recently near Jupiter (Grard *et al* 1977), were shown to be caused by the collection of spacecraft-emitted electrons.

Several authors discussed the effects of differentially charged insulators on electric-field experiments on spacecraft. The probe method of measuring electric fields uses two separated probes where each comes to an equilibrium floating potential with respect to the local plasma. The difference in the floating potentials is proportional to the electric field. A high degree of symmetry is required in the potential distribution around the spacecraft to ensure that the charging currents to each probe are identical. Soop (1972, 1973) showed that exposed insulators could charge differently than the spacecraft and produce large asymmetries in the potential distribution. Cauffman (1973a) and Cauffman and Maynard (1974) showed that photoelectron space charge in the photosheath could also produce asymmetric potential distributions. However, a dielectric surface emitting electrons uniformly tends to be an equipotential as if the surface were conducting, because of the transverse motion of the electrons (e.g. De 1979).

Fahleson (1973) predicted that a spacecraft with an insulating surface which charges to a highly negative potential on the dark side will have a potential barrier produced adjacent to the sunlit side. This will prevent photoelectrons from escaping from the sunlit side with the consequence that the whole spacecraft will come to a more negative potential than it would have otherwise. This effect has been confirmed by detailed current balance calculations (e.g. Mandel *et al* 1978) and observed on the ATS-6 satellite (see below). Besse and Rubin (1980) have shown that a simple analytic model for the potential distribution consisting of monopole and dipole terms can be used for analysing charging effects when a potential barrier is involved.

6.2. Observations implying differential charging

Observations of differential charging on spacecraft have almost all been indirect because of the difficulty of measuring directly the potential of an insulating surface. However,

there have been experiments on the SCATHA spacecraft which measured directly the electric field due to charges on a dielectric surface (Mizera *et al* 1979). DeForest (1973) inferred differential potentials of several kV on ATS-5 from modulations of ion counts by the satellite spin. Fredricks and Scarf (1973) performed a detailed analysis on anomalies observed on a number of synchronous-orbit satellites. The flight data, together with laboratory simulations, led to the conclusion that portions of the spacecraft surfaces charged to many kV negative during magnetic substorms and that these surfaces were frequently discharged by arcs or coronas. Scarf *et al* (1974) detected noise in wave experiments on Imp 7 that was associated with the rotation of the sixteen-sided, insulated spacecraft. As each side rotated into shadow or sunlight, there were current transients producing fluctuating magnetic fields. Modulation of the sheath was also detected by the electric dipole antenna. Cauffman (1973b) found a correlation between spacecraft anomalies and geophysical parameters, and Cauffman and Shaw (1975) proposed a simple coupling model to explain the response of electronic circuits to electric discharges on a satellite. Shaw *et al* (1976) flew an experiment on a satellite in synchronous orbit to study differential charging and to detect dielectric breakdown. Two kinds of discharges were observed: one was spin-synchronous and the other occurred near local midnight during magnetic substorms.

Considerable data on differential charging have been obtained from the ATS-6 spacecraft. Frequently, low-energy electrons detected at a few eV were photoelectrons and/or secondary electrons coming from the spacecraft surface. Figure 14 from Whipple (1976a) shows a typical electron distribution function with a transition energy at about 40 eV between the photoelectrons and plasma electrons, which implies the existence of a potential barrier of about 40 V about the spacecraft. It was shown that a potential barrier as high as tens of volts could not be explained as a space charge effect, a mechanism

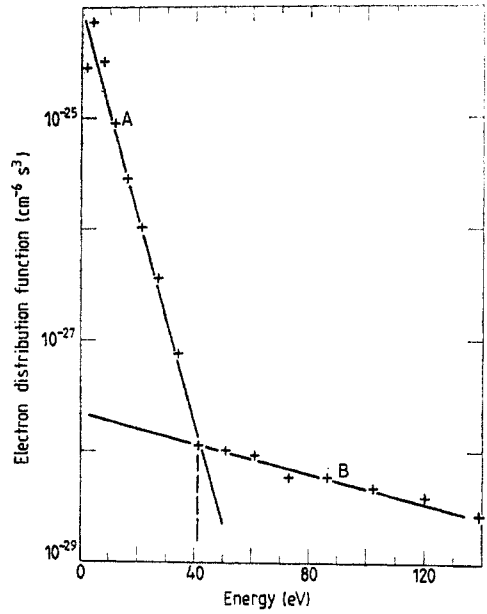

Figure 14. Electron velocity distribution plotted against energy showing photoelectrons returned to the spacecraft by a potential barrier (Whipple 1976a). A, $T \cong 4.9$ eV, $n \cong 10$ cm^{-3} if source is spacecraft, 610 cm^{-3} if ambient. B, $T = 65$ eV, $n = 0.2$ cm^{-3}.

suggested earlier by others (e.g. Guernsey and Fu 1970, Fu 1971, Tunaley and Jones 1973) but must instead be caused by differential charging (Whipple 1976b).

Figure 15 (plate) is a particle spectrogram from ATS-6 showing both ion and electron data for a period of 2 h on 8 September 1974. The energy scale is on the vertical axis with zero in the middle; the intensity of the shading is a measure of the particle count rate, with high count rates white and low count rates dark. The spacecraft is in eclipse from 5:57 to 6:31, and during this time the spacecraft potential goes as high as -8 kV, as can be seen by the absence of ions with energies below about 8 keV. The intense band of electrons below about 60 eV after eclipse is exited is made up of photoelectrons reflected back to the satellite from a potential barrier. The modulation of the top of this band of electrons is caused by the rotation of the detector. It can see higher-energy photoelectrons when looking tangential to the spacecraft surface than when looking perpendicular. The potential distribution after the eclipse when the main body was at about -80 V was obtained by Olsen *et al* (1981) from a solution of Laplace's equation. They found that a potential of about -300 V on the large, shadowed, dielectric antenna would produce a potential barrier of 60 V for electrons, as shown in figure 16.

6.3. Discharge processes

The occurrence of anomalies in the behaviour of spacecraft systems has led to laboratory investigations of discharge processes of materials in a vacuum. The studies involve irradiation of typical spacecraft materials with energetic electrons and measurements of the discharge properties. A brief description is given here of the current understanding of the discharge process; the interested reader is referred to papers in the proceedings of the three spacecraft charging technology conferences (Pike and Lovell 1977, Finke and Pike 1979, Pike and Stevens 1981). The discharge process is complicated and not yet well understood because of its dependence on material properties, especially on microscopic imperfections such as cracks, holes, etc, and on the macroscopic configuration such as grounding arrangements and proximity of other materials, etc.

The physical picture of what happens in a discharge is that incident electrons penetrate a dielectric material, forming a space charge layer at a depth of the order of microns below the surface. As the electric field within the material increases, a critical value is eventually reached where breakdown of the material occurs accompanied by material vaporisation and ionisation. A discharge is initiated which propagates across the surface or through the material, removing the bound charge and capturing it into the discharge. Discharges frequently seem to originate in holes, cracks, seams, or at the edges of material where presumably the electrical stress is larger. Meulenberg (1976) has suggested a bilayer mechanism for some discharges where the negative space charge layer at a depth of microns is accompanied by a positive layer nearer the surface at a depth of some tens of ångströms due to secondary electron emission or photoemission. If the bulk resistivity of the material is sufficiently high, there can be breakdown initiated within the bilayer. Yadlowsky *et al* (1979) have shown that if the edges of the material are shielded from the incident electron fluxes, the breakdown electric field can be much higher. Under these conditions a puncture discharge can occur through the material with the entire sample surface discharged by lateral currents flowing beneath the surface.

Discharges can also occur from metal to metal, metal to dielectric, dielectric to metal and dielectric to space (Hoffmaster and Sellen 1976, Inouye and Sellen 1978). A mechanism for this latter charge blowoff phenomenon has been suggested by Leadon and Wilkenfeld (1979) involving the effect of the $\boldsymbol{V} \times \boldsymbol{B}$ force on electrons moving towards a

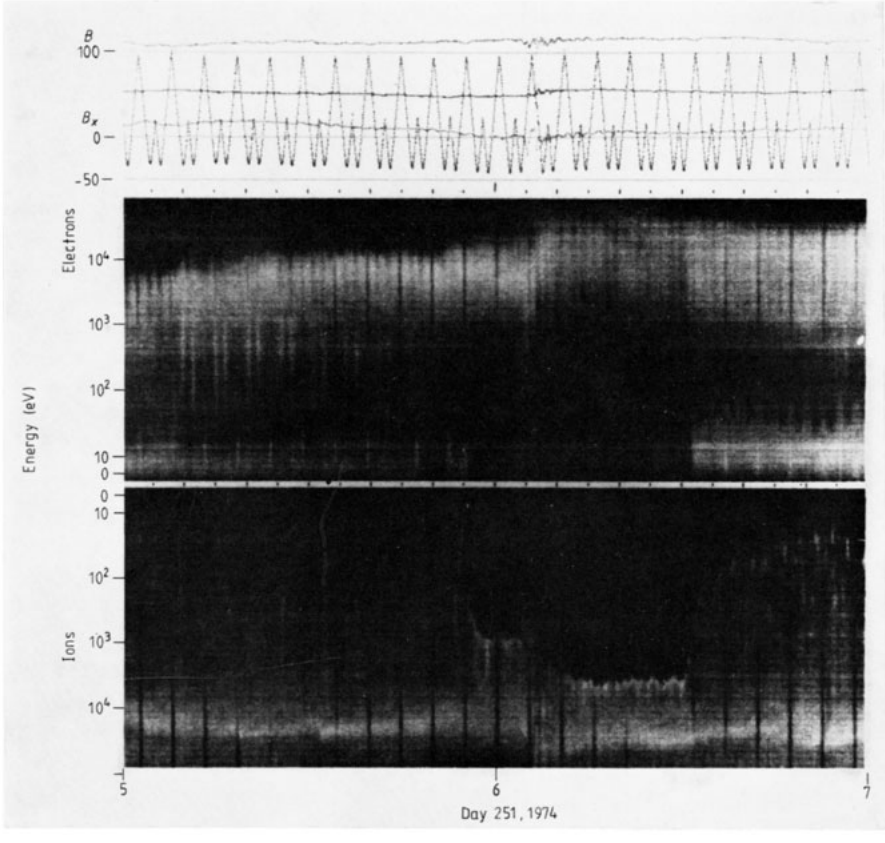

Figure 15. Spectrogram of ATS-6 particle data for 8 September 1974. The spacecraft potential is indicated by the absence of ions (dark regions) below a threshold energy where the count rate rises abruptly (bright areas). The spacecraft is in eclipse from 5:57 to 6:31. Note that the energy scale increases upwards for electrons and downwards for ions.

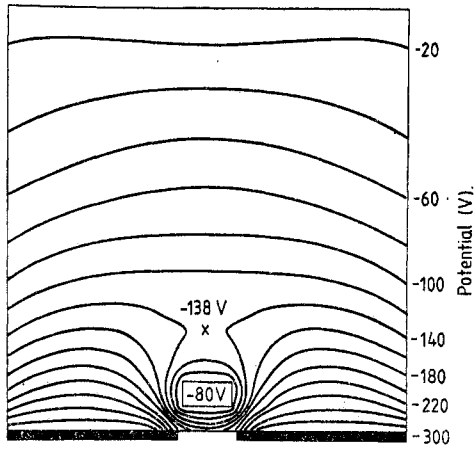

Figure 16. Potential contours from a solution of the Laplace equation for a model of the ATS-6 spacecraft, with boundary conditions of -80 V on the box representing the experiment module and -300 V on the dielectric antenna plate. A saddle point is formed over the box at -138 V representing a potential barrier for electrons with energies less than 58 eV (Olsen *et al* 1981).

punchthrough or flashover point. Irradiation by ultraviolet light can drain off charges by photoconduction and thus reduce the frequency of discharges, but it may also trigger discharges by removing surface electrons through photoemission and enhancing the bilayer electric field (Meulenberg 1976). A study of breakdown on second-surface mirrors found discharge pulse risetimes of 0.02 μs and pulse lengths of 1 μs (Adamo and Nanevicz 1976). Low potentials on very thin surface films can lead to 'Malter' breakdown where the small potential drop across layers such as optical coatings or oxide layers leads to large electric fields. The breakdown results in light scintillations and radio noise (Malter 1936, Nanevicz and Adamo 1976).

Comparatively large surface areas of dielectrics can be cleaned off in a single discharge. If the surface gradient is large enough, an avalanche can occur caused by secondary electron multiplication leading to a propagating discharge wave (Inouye and Sellen 1978). Balmain (1979, 1980) has shown that there are scaling laws relating the characteristics of a discharge to the surface area that is discharged. The scaling laws can be explained by a discharge propagating at a constant velocity which in Balmain's experiments was of the order of 3×10^5 m s^{-1}. For a given surface charge density, $\sigma=\mathrm{d}Q/\mathrm{d}A$, the current increases linearly with time: $I=\sigma\,\mathrm{d}A/\mathrm{d}t=\sigma v^2 t$. The peak current is proportional to the pulse length $\tau=r/v$, where A is the area, r is the linear dimension of the surface and v is the propagation velocity. Thus both the peak current and the pulse length scale as $A^{1/2}$, whereas the charge that is cleared scales as A and the energy released scales as $A^{3/2}$. Peak currents exceeding 100 A have been observed in some laboratory discharge experiments (Inouye and Sellen 1978). The discharge does not propagate uniformly through the material but rather through filamentary tracks which leave a network of damage tunnels and cracks in what is known as a Lichtenberg pattern.

7. Measurements of potential

7.1. How potentials are measured

Spacecraft potentials are for the most part inferred from their effect on data obtained with charged-particle measurements. Both spherical and cylindrical Langmuir probes

have been flown on a great number of spacecraft to obtain ion and electron densities and temperatures and also ion mass (e.g. Brace *et al* 1973). The spacecraft potential is inferred from the shift of the current–voltage curve along the voltage axis. As the potential on the probe with respect to the plasma goes through zero, there is an inflection point in the curve as can be seen from equations (3.2) and (3.3). Bowen *et al* (1964) suggested an electronic implementation of Druyvesteyn's analysis (1930) where the second derivative of the current–voltage curve shows a sharp spike at the probe voltage corresponding to zero volts with respect to the plasma. This method was used on Ariel 1 (Samir and Willmore 1966) and also on rocket flights (Bering *et al* 1973).

Both spherical ion and electron traps (e.g. Gringauz 1963, Sagalyn and Burke 1977) and planar retarding potential analysers (e.g. Knudsen 1966, Hanson *et al* 1970, Whipple *et al* 1974) have been flown on a number of spacecraft. Most of these instruments make use of the streaming velocity of the ions in the spacecraft reference frame to infer the vehicle potential from the retarding potential that it takes to cut off the ion current. Thus in the ionosphere where O^+ is the dominant ion, the orbital velocity of the spacecraft gives the ion a kinetic energy of about 5 eV. The shift from 5 V of the retarding potential that it takes to cut off the ion current is then a measure of the spacecraft potential. The angle of attack of the instrument, the thermal spread in ion velocities, and in some cases the effect of ionospheric winds also have to be considered (Hanson and Heelis 1975).

Differential techniques essentially measure the velocity distribution function of the particles for a given energy and direction. The shift of the distribution functions in energy is one way of inferring the vehicle potential. In addition, there will be no attracted particles present at the spacecraft from the plasma at energies below the potential energy through which the particles have fallen. Both of these effects can be seen in figure 17,

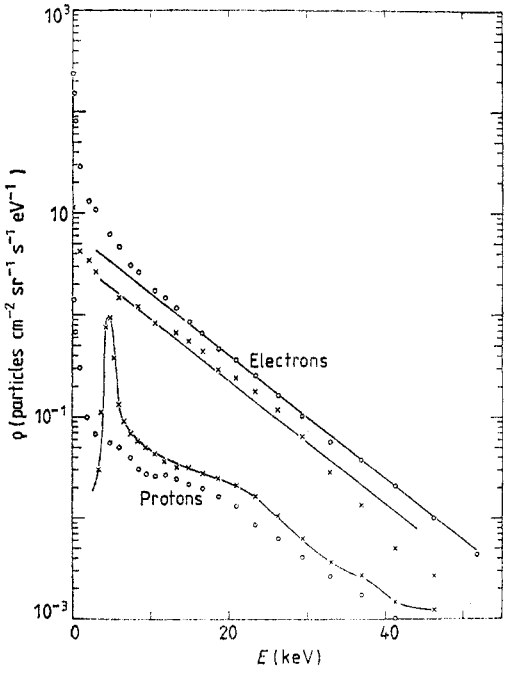

Figure 17. Phase space density of particles before and during eclipse showing the effects of charging to −4.2 kV in eclipse (DeForest 1972). ○, pre-eclipse; ×, eclipse.

taken from DeForest (1972), where he first reported large spacecraft potentials of several kV at synchronous orbit. As the spacecraft entered eclipse the spacecraft potential shifted 4.2 kV negative, and the ion and electron spectra shifted by this amount in opposite directions. There are no ions present with energies below 4.2 keV during eclipse; the large spike of ions just above this energy is caused by the acceleration of all low-energy ions into the first energy channel of the analyser above 4.2 keV.

Although positive spacecraft potentials can in principle be inferred through the absence of plasma electrons below an energy equivalent to the spacecraft potential, in practice this is difficult because of the presence of photoelectrons and secondary electrons at low energies. At times the difference in spectral shape between plasma electrons and spacecraft-emitted electrons can be used to distinguish between them (e.g. Fahleson 1973, Rosenbauer 1973), but care must be taken that differential charging and potential barriers are not present which can lead to incorrect inferences of the spacecraft potential. Deliberate emission of charged particles by devices such as plasma generators, ion or electron accelerators, or through thermal electron emission can also be used to measure vehicle potentials by detecting the energy it takes for particles to escape.

Changes in spacecraft potential can sometimes be measured by detecting the change in potential difference between a floating probe, such as an electric-field antenna, and the spacecraft. This technique has been used during experiments where ion or electron beams were emitted in order to deliberately change the spacecraft potential (e.g. Cohen 1981).

7.2. Measurements of spacecraft potential

The predictions of satellite potential in the ionosphere were of negative values of the order of a few times the equivalent electron temperature. The first satellite results were from Sputnik 3 indicating potentials from -2 to -6 V depending upon altitude and position in orbit (Krasovskii 1958, Gringauz *et al* 1961). These relatively large negative potentials led to speculation that the electron temperature in the ionosphere could be as large as 1 or 2 eV (i.e. 1 or 2×10^4 K). Such large electron temperatures did not seem compatible with accepted ideas of the formation and structure of the ionosphere or with radio measurements which indicated electron temperatures of at most only a few tenths of an eV.

This discrepancy began to be resolved when the Explorer 8 satellite was launched in 1960, carrying a number of experiments for evaluating the various charging currents to the spacecraft and for measuring the equilibrium potential. Negative potentials of a few tenths of a volt were obtained, in reasonable agreement with predicted values (Brundin 1963, Whipple 1965). As other measurements of potential came in from other spacecraft over the next few years, it became apparent that the potentials fell into three classes: large negative potentials of up to a few tens of volts; 'normal' potentials of a few tenths of a volt negative for spacecraft in the ionosphere; and positive potentials of a few volts observed for the most part on spacecraft that went to great distances from the Earth into the outer magnetosphere or into the solar wind. A number of these measurements are shown in table 3. Most satellites with large negative potentials turned out to have either long antennae or surfaces with positive potentials exposed to the plasma, such as solar arrays. These surfaces acted as electron collecting electrodes either because of the positive potential or because of the induction effect described by Beard and Johnson (1960) in the long antennae. The large electron currents to these surfaces drove the space-

Table 3. Some measurements of satellite potential.

Satellite	Launch date	Experiment	Satellite potential and comments
Sputnik 3	15/5/58	Ion traps	Negative to −6 V
Explorer 8	3/11/60	Ion and electron traps	Normal†. No solar cells, some effect from RF probe
Discoverer 32	13/10/61	Ion trap	Normal†
Cosmos 2	6/4/62	Langmuir probe and ion traps	Negative potential increased by positive potentials on outer grids of traps
Air Force Satellite	17/4/62	Ion trap	Negative to −20 V
Ariel 1	26/4/62	Langmuir probes	Normal† up to −1.0 V
Explorer 17	3/4/63	Langmuir probe	Normal† up to −1.0 V at night
Tiros 7	19/6/63	Langmuir probe	Normal†. Negative solar cells
IMP A (Explorer 18)	27/11/63	Electron trap	1–2 V positive, positive solar cells
Explorer 20	25/8/64	Langmuir probe	Negative to −8 V, positive solar cells
OGO 1	5/9/64	Ion and electron traps, mass spectrometer	Negative to −15 V, positive solar cells
IMP B (Explorer 21)	4/10/64	Electron trap	1–2 V positive, positive solar cells
Explorer 22	10/10/64	Langmuir probe	Negative, exceeding −4 V at times. Some positive solar cells
Explorer 27	29/4/65	Langmuir probe	Negative to −8 V. Some solar cell terminals coated
IMP C (Explorer 28)	29/5/65	Electron trap	1–2 V positive, positive solar cells
OGO 2	14/10/65	Ion and electron traps, mass spectrometer	Negative to −3 V, solar cell terminals coated

† 'Normal' means a few tenths of a volt negative near the Earth.

craft to a more negative potential than it would have otherwise attained. The positive values at the higher altitudes were a result of the effects of photoemission.

Potentials as high as several tens of volts negative have been reported for spacecraft in the ionosphere as they go through the auroral zones (Knudsen and Sharp 1967, Sagalyn and Burke 1977). These potentials were undoubtedly caused by large fluxes of energetic electrons coming down magnetic-field lines during times of auroral activity. Parks and Katz (1981) have pointed out that large spacecraft in such environments might charge to very large potentials because the electron current must be balanced by the ion ram current which increases very slowly with spacecraft potential due to the small ratio of Debye length to body size.

In addition to the high negative spacecraft potentials of several kV reported by DeForest (1972, 1973) for ATS-5 at synchronous altitude in the magnetosphere, large potentials have also been observed on ATS-6 in both eclipse conditions and in sunlight (Johnson *et al* 1978, Garrett and DeForest 1979). Figure 18 (plate) from Olsen and Purvis (1981) shows in spectrogram format the record potential of -19 kV which was observed on ATS-6 on 8 October 1975. There have been a great number of satellites stationed in geosynchronous orbits but only a few of these have had instrumentation for measuring spacecraft potentials. The SCATHA spacecraft has observed potentials as large as -8 kV during eclipse, but the European spacecraft GEOS 2 observed a maximum potential of only -1.5 kV. The difference in behaviour between GEOS 2 and the ATS and SCATHA spacecraft is quite likely due to the effort spent to ensure electromagnetic cleanliness on GEOS.

Cauffman (1974) reported positive potentials of more than 15 V on IMP 6 during injections of energetic electrons into the magnetosphere during substorms and attributed this to differences in photoemission and secondary electron emission properties of the spacecraft surface materials. Montgomery *et al* (1973) reported potentials as high as $+70$ V on Vela 5 and Vela 6 in the Earth's magnetotail, but it is possible that these were actually observations of potential barriers due to differential charging.

Ogilvie *et al* (1977) observed positive potentials as large as 100 V on Mariner 10 during encounters with the planet Mercury, particularly as the spacecraft went through the polar regions where the plasma fluxes were low. Unusual potentials have not been reported on spacecraft missions to Mars or Venus. Scarf (1976) has inferred charging of the Pioneer spacecraft in Jupiter's magnetosphere through interference phenomena observed with plasma wave detectors, but as yet there have been no definite measurements of potentials reported for these spacecraft in the magnetospheres of either Jupiter or Saturn although high potentials are likely (however, see Scudder *et al* 1981).

8. Potential modification and control on spacecraft

8.1. Reasons for potential modification and control

The initial stimulus for investigating methods for changing and eventually controlling spacecraft potentials was the interfering effect of spacecraft charge on low-energy particle and electric-field experiments. It proved especially difficult to obtain reliable measurements of low-energy particles in the Earth's magnetosphere and it is only quite recently that detailed information on the 'thermal' population, i.e. particles at or below a few eV, has begun to emerge (e.g. Decreau *et al* 1978, Chappell *et al* 1980). These recent advances have been made largely because of the recognition of spacecraft charging effects and the implementation of charging control measures, especially by European groups in the construction of the GEOS 1 and 2 and ISEE spacecraft. Only the ability

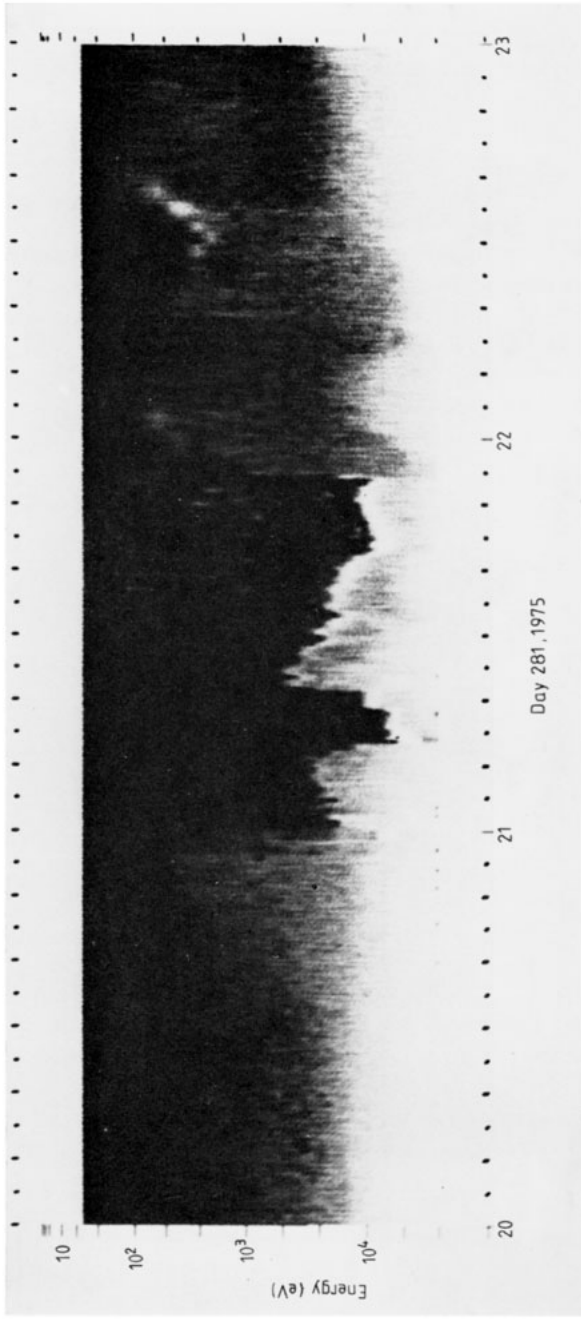

Figure 18. Spectrogram of ATS-6 ion data on 8 October 1975 showing a record spacecraft potential of −19 kV at about 21:14 UT. The potential is inferred from the absence of counts (dark areas) below a threshold energy equivalent to the spacecraft potential where the count rate rises abruptly (bright areas).

to maintain the spacecraft potential very close to zero volts, or the use of means to swing the potential artificially a few volts during quiet conditions, has made possible the detection of certain low-energy populations (Wrenn *et al* 1979a, Olsen 1980).

Another stimulus for controlling spacecraft potentials was the use of electron beams on space vehicles for experimental purposes such as the generation of artificial aurorae, magnetic conjugate studies and plasma physics investigations. Ejection of the electron beam tends to drive the vehicle positive and thus reduce the energy of the beam electrons and perhaps prevent their escape. Successful experiments require a neutralising return current of electrons (or emission of positive charge) to keep the vehicle potential near zero. Thus the rocket carrying the first electron beam experiment had a large aluminised Mylar foil for collecting returning electrons. In spite of a partial failure of the deployment system, there was no evidence of large potentials on the rocket because of large fluxes of heated electrons from the ionosphere to the rocket body and partially deployed foil (Hess *et al* 1971). A number of other groups have since carried out similar experiments. This work has been recently reviewed by Winckler (1980) (see also Jacobson and Maynard 1980, Arnoldy and Winkler 1981) who has an extensive discussion of the neutralisation process at ionospheric altitudes. The vehicle, emitted beam, return currents and the ambient magnetic plasma medium must be considered as an interacting system. There is a beam–plasma 'discharge' which produces large numbers of heated electrons in the vicinity of the spacecraft by a variety of processes, probably including collisional ionisation of the ambient and vehicle-produced neutral gases, secondary electron production, and the effects of waves and instabilities excited in the surrounding plasma.

The third incentive for development of spacecraft potential control techniques was the occurrence of spacecraft system anomalies associated with charging events. There are basically two approaches: the first involves *passive* techniques such as the development of special surface materials and an emphasis on 'electrostatic cleanliness' where the exposure of insulators on the surface is minimised; and secondly, *active* techniques involving the use of charged-particle emitters to change the total charge and its distribution on the spacecraft.

8.2. Passive methods

Recognition of possible harmful effects of charging has led to the concept of requiring 'electrostatic cleanliness' for spacecraft. Ideally, one would like to have complete elimination of exposed insulating materials and common grounding of the exposed conducting surfaces so that differential charging is not present. In practice, complete elimination of insulators is not possible because of the need for isolated elements such as antennae, particle collectors, etc. Consequently, a set of criteria has evolved which specify the conductivity of exposed surfaces and the magnitude of allowed potential differences between spacecraft elements based on the particular mission. These specifications were originally developed during the design phases of the ISEE and GEOS spacecraft and appear to have been quite effective; the most negative potential reached by GEOS 2 was -1500 V in eclipse which is much less than potentials reached by ATS-5 and ATS-6 (Wrenn 1979, Wrenn *et al* 1979b).

The need for conducting surfaces on spacecraft has stimulated a large research effort in both measuring the properties of typical surface materials as well as the development of new materials. The use of selected materials with high secondary electron emission yields has been proposed to help avoid high negative equilibrium potentials (Knott

1972, Rubin *et al* 1978). The desired electrical properties of high secondary and photoemission yields and good conductivity are frequently incompatible with other desired surface properties such as low thermal conductivity or good optical transparency. Lehn (1977) has reviewed some of the recent development of special materials such as conductive polymers, paints, transparent films and coatings as well as fabric interweaves.

The occurrence of anomalies on spacecraft can be minimised by appropriate protective measures, such as electrostatic shielding, redundant or hardened components for sensitive circuits, and proper grounding techniques. Reiff *et al* (1979) and Parker and Oran (1979) suggested that large structures in space such as solar power satellites might be protected from energetic charged particles by magnetic shielding, similar to the way in which 'Spacecraft Earth' is protected from the hazards of cosmic rays. Grard (1975, 1976) has suggested that negative potentials can be limited by means of a field emission probe consisting of sharp-pointed filaments electrically connected to the spacecraft.

8.3. Active methods

Other ways of modifying the current balance to a rocket or satellite are to artificially enhance the ambient fluxes or generate new currents between the vehicle and the plasma. Charging currents can be influenced by the appropriate biasing of exposed surfaces or the emission of neutral gas which is subsequently ionised (e.g. Israelson and Winckler 1979). However, the most obvious method for actively controlling spacecraft potentials is through the emission of charged particles by means of accelerators or plasma emission devices. It might be thought that emission of electrons would be a simple but effective means of reducing large negative potentials, but emission of only electrons can be more hazardous than helpful. The ejection of electrons can create large potential differences between insulators which retain their previous charge and the spacecraft ground, which is suddenly changed to a more positive potential. This actually happened on the SCATHA spacecraft, resulting in a partial failure of one of the particle experiments during operation of the electron beam experiment (Cohen 1981). Arcing was detected by pulse monitors and there were also transient problems in the telemetry system. A similar effect could occur on the proposed Shuttle orbiter (Liemohn 1976, 1977).

There have only been a few experiments involving charged-particle emission where modification of the spacecraft potential was the primary aim. Almost all of the ionospheric experiments involving electron beams (Winckler 1980) were carrying out environmental investigations and the vehicle charging effects were incidental. However, Cohen *et al* (1979a, b) emitted both positive ions and electrons from an ionospheric rocket and charged the vehicle to 1 kV during the emission of 400 A of 2 keV positive xenon ions. The potential varied with altitude in a manner suggesting dependence on the ambient plasma density but independent of neutral density and vehicle orientation.

Experiments aimed at modifying vehicle potentials in the magnetosphere have been carried out on ISEE 1, ATS-5 and ATS-6, and the SCATHA spacecraft. In none of these experiments was there any evidence for the kind of beam–plasma discharge which characterised electron emission experiments in the ionosphere. The difference must be ascribed to the very low plasma and neutral densities in the environment at magnetospheric altitudes compared to the ionosphere. The ISEE 1 experiment (Gonfalone *et al* 1979) used electron guns capable of emitting currents between 10^{-8} and 10^{-3} A at energies from about 0.6 to 41 eV. They were able to stabilise the vehicle potential at a value more positive than the normally positive floating potential and were also able to reduce the spin modulation of the spacecraft potential.

The ATS-5 and ATS-6 investigations were carried out with experimental caesium ion thrusters on the spacecraft. Each thruster had a separate electron emitter for neutralising the ion beam, consisting of either a hot wire filament (ATS-5) or a low-energy plasma generator (ATS-6). Operation of the ATS-5 electron emitter reduced the magnitude of large negative potentials in eclipse but rarely discharged the spacecraft completely (Bartlett *et al* 1975, Goldstein and DeForest 1976). Olsen (1980) showed that at equilibrium less than 1% of the emitted electron current was escaping the spacecraft because differential potentials of the order of 100 V developed on dielectric surfaces (e.g. solar cells) creating potential barriers.

Slow charging and discharging rates sometimes observed on both ATS-5 and ATS-6 during beam operations were explained by Purvis (1980) and Olsen (1980) as a result of differential charging of dielectrics with high capacitances. The ATS-6 plasma emitter and ion engine were both able to discharge large negative potentials (Goldstein and DeForest 1976, Purvis *et al* 1977, Bartlett and Purvis 1979), but the plasma neutraliser was only able to reduce differential charging and not eliminate it. It proved possible to use the thruster in active environments to hold the spacecraft to about -5 V (determined by the beam to spacecraft bias) and to prevent charging of the dielectric surfaces. The ATS-5 and ATS-6 experiments have been reviewed by Purvis and Bartlett (1980).

Preliminary results from the SCATHA emitter experiments (Cohen 1981) indicate that it has been possible to discharge large negative potentials and also charge the vehicle to either positive or negative potentials by an appropriate combination of ion and/or electron beam currents and energies.

Active potential control systems have been suggested for interplanetary spacecraft (Kawashima 1972) and for spacecraft in Jupiter's magnetosphere (Beattie and Goldstein 1977) but no schemes have yet been implemented.

9. Astrophysical applications

9.1. Interplanetary and magnetospheric dust

Some of the consequences of electrostatic charging of astrophysical bodies have been touched on in the previous sections. In this section, a brief survey is made of observations and inferences of astrophysical charging effects, beginning with work in the solar system. Mendis (1981) has recently reviewed the role of electrostatic charging of small and intermediate sized bodies in the solar system (see also Brownlee 1979).

The charging of dust grains in the solar system affects both the motion of grains through electromagnetic forces and their size through electrostatic disruption. Dust grains in the solar wind charge to about $+10$ V and are subject to the polarisation electric field of the solar wind and the Lorentz force (Parker 1964, Parthasarathy 1978). (These forces can be combined into the expression: $q(\boldsymbol{v}-\boldsymbol{V})\times\boldsymbol{B}$, where $\boldsymbol{V}$ is the solar-wind velocity and $\boldsymbol{v}$ is the grain velocity.) Changes in the direction of $\boldsymbol{B}$ due to the solar-wind sector structure of the interplanetary field lead to velocity perturbations, and variations in the size of sectors lead to a diffusive or random-walk motion of the grains and a spread in their orbital parameters (Consalmagno 1979, Hughes 1980). Morfill and Grun (1979a) find that these stochastic variations tend to shift the plane of symmetry of the zodiacal dust cloud toward the solar magnetic equator inside 1 AU, whereas outside 10 AU there is no such systematic effect. Inside about 0.3 AU there can be resonant orbits where the orbital period is comparable to twice the solar rotation period, and consequently rapid changes in the dust grain orbits are possible. These authors also show (Morfill and

Grun 1979b) that interstellar grains can penetrate deep into the solar system only if they are bigger than 0.1 μm, and even then their penetration depends on their latitude and the direction of the magnetic field.

The motion of charged dust grains in planetary magnetospheres has been discussed by Mendis and Axford (1974), Hill and Mendis (1979, 1980), Morfill *et al* (1980a) and Consalmagno (1980). Within the region of the magnetosphere where the plasma is co-rotating, the plasma polarisation electric field induced by the co-rotation must be taken into account. The sense of the co-rotation electric field at Jupiter and Saturn is such as to attract negatively charged grains, whereas at Earth the field is repulsive. Hill and Mendis (1980) computed the orbits of grains injected into Jupiter's magnetosphere and found that the grains could be trapped into stable orbits at about 2 Jovian radii. The long charging times for the grains meant that the potentials had to be calculated as a function of time. The calculated dust distribution seems to be in reasonable agreement with the thin dust ring observed by the Voyager 1 spacecraft (Smith *et al* 1979) and the enhanced dust flux observed by Pioneer 10 (Humes *et al* 1975). Johnson *et al* (1980) and Morfill *et al* (1980 b, c) argue that Jupiter's satellite Io may also be a source of charged dust. Hill and Mendis (1979) have suggested that the brightness asymmetries of Jupiter's Galilean satellites might be explained by the impact geometries of charged micrometeoroids on their surfaces.

Fechtig *et al* (1979) observed 'bursts' of micrometeoroids within 10 Earth radii from the HEOS 2 spacecraft. They classified the bursts into 'swarms' and 'groups' according to the time between events. Groups had intervals less than 6.5 h and duration from 50 min to 13 h and were thought to be particles ejected from the lunar surface by meteorite impact. Swarms had intervals less than 10 min and duration less than 40 min and were believed to be caused by electrostatic disruption as the parent bodies went through the hot plasma in the auroral regions of the Earth's magnetosphere. It is not likely that large bodies ($> 10^2$ g) can be disrupted in this way, but smaller bodies (< 10 g) with low tensile strength such as very loose dust balls ($F_t \cong 10^3$ dyn cm^{-2}, see equation (3.22)) could be disrupted by potentials of a few hundred V. Such disruption probably also occurs in the magnetospheres of Jupiter and Saturn.

The very recent Voyager 1 encounter with Saturn produced intriguing observations of Saturn's rings indicating possible electrostatic charging effects on smaller dust particles. The outer F ring was observed to have a wavy, braided configuration. 'Spokes' were observed in the B ring primarily below synchronous altitude and appeared to be triggered by some mechanism on the midnight side of Saturn. The observations in forward and back-scattered sunlight indicated that the F ring and spokes were both composed of micron-sized grains. If there were sudden charging on the midnight side of Saturn, as there is at Earth, then the additional force due to the combined co-rotation electric field and Lorentz force increases strongly inwards from synchronous orbit. Hill and Mendis (1981) suggest that the F ring configuration could be due to the Lorentz force imparting a gyro-motion to the grains causing an oscillation back and forth about a circular orbit. Additional evidence for charging in the rings was the observation of radio noise by the Voyager 1 radio astronomy experiment at frequencies too low to have originated at Saturn's surface and penetrated Saturn's ionosphere (Warwick *et al* 1981).

Ip (1979, 1980) has shown that particles in the rings of Saturn are an important loss mechanism for H^+ and an important source for H. The rings of both Jupiter and Saturn were observed by the Pioneer spacecraft through their depletion effects on energetic charged particles (Fillius *et al* 1975, 1980), and Morfill *et al* (1980d) have suggested that the dust in Jupiter's magnetosphere significantly depletes the Jovian plasma.

9.2. The lunar surface

Early ideas that charging could lead to transport of lunar dust (see §2.1) have been confirmed by observations on the lunar surface (Gold and Williams 1973). Berg *et al* (1974, 1975) reported enhancements by two orders of magnitude in dust impacts to the Lunar Ejecta and Meteorites Experiment at sunrise for detectors looking east and up, implying that particles were moving away from the terminator. They inferred that the impacts were due to slowly moving but highly charged lunar fines. The events clustered preferentially around sunrise but there was a peak at sunset as well.

Criswell (1973) and Rennilson and Criswell (1974) described photographs from the Lunar Surveyor spacecraft showing a horizon glow following sunset which they suggested was due to light scattering from dust at altitudes between 3–30 cm above the lunar surface. They inferred a line-of-sight density of 50 cm^{-2} of 10 μm size particles in a temporary tenuous cloud above sharp sunlight/shadow boundaries. De and Criswell (1977) and Criswell and De (1977) have argued that there can be intense 'supercharging' in terminator regions as the areas of sunlit regions decrease, resulting in an intensification of local electric fields. However Gault *et al* (1970) argued that the horizon glow may be due to refraction rather than scattering by dust particles above the surface. The crew of Apollo 17 saw streamers accompanying spacecraft sunrise at altitudes as high as 100 km above the lunar surface which McCoy and Criswell (1974) also interpreted as being caused by light scattering from lunar dust of 0.1 μm size. Rhee (1976) has discussed the electrostatic disruption of lunar dust particles. Gold *et al* (1979) measured secondary electron emission characteristics of lunar soil samples and argued that the differing yield with depth may be evidence for deposition by electrostatic transport.

The early estimates of lunar surface potentials of a few volts positive for the sunlit surface in the solar wind (see §2.1) were extended by Manka (1972, 1973). He calculated potentials as a function of solar zenith angle for various photoyields and obtained subsolar values from 0 to about +20 V. The potentials went to negative values at the terminator and on the dark side could be as negative as −1800 V, depending on secondary emission yields and on the incident ion fluxes. He calculated ion fluxes based on ionisation of mainly heavy atoms such as Ne, Ar and Kr in the lunar atmosphere and their subsequent acceleration to the surface. Fenner *et al* (1973) and Freeman *et al* (1973a, b) obtained potentials of about +10 V for solar zenith angles between 25° and 45° from particle experiments on the Moon's surface while the Moon was in the solar wind and Earth's magnetosheath. The potentials were inferred from an analysis of the energy spectrum of ions from the lunar ionosphere. Goldstein (1974) inferred somewhat lower potentials for the subsolar point (from −3 to +5 V) based on observation of electrons. He suggested that the potential variation above the surface was not monotonic, but that there was a potential barrier for electrons of a few volts caused by the photoelectron space charge. Both Goldstein (1974) and Reasoner and Burke (1972, 1973) inferred somewhat higher photoelectron yields for the lunar surface material than had been obtained from laboratory measurements (Willis *et al* 1973a, b). Reasoner and Burke (1972, 1973) found that the sunlit surface while the Moon was in the geomagnetic tail could be at a potential as high as +200 V because of the low density of the plasma in this region. Lindeman *et al* (1973) inferred a potential of −100 V at the terminator, and Benson (1977) found potentials of about −50 V in a region between 20°–30° from the terminator on the sunlit side.

9.3. Other solar-system bodies

Other bodies in the solar wind with little or no atmosphere of their own should have

surface potentials similar to the Moon's. Mendis *et al* (1981) have suggested that water-dominated comets beyond 5 AU from the Sun will not have a protective atmosphere and thus may charge to potentials such that submicron dust particles could be electrostatically levitated and blown off the cometary surface. This might explain periodic dust outbursts which have been observed from some distant comets, since the potentials on the dark side of the comet would be modulated by the solar-wind speed. This mechanism could also provide a source of fine dust in the outer solar system.

A spectacular example of a combination of electrostatic and induced electric fields may occur in the interaction of Jupiter's satellite Io with Jupiter's magnetic field. Decametric radio emissions from Jupiter are significantly modulated by the satellite Io. Gurnett (1972) suggested an interaction model where the $\boldsymbol{V}\times\boldsymbol{B}$ electric field due to Io's motion sets up a potential difference across Io and its ionosphere approaching 600 kV. This EMF drives currents in the circuit consisting of Io's ionosphere, the flux tubes joining Io to Jupiter, and Jupiter's ionosphere; the EMF also results in plasma sheaths between Io's ionosphere and the plasma in Jupiter's magnetosphere. The potential drop across the sheaths depends on the position about Io and can be of either polarity, resulting in acceleration of ions and electrons both to and from the satellite. These ideas were further developed by Shawhan *et al* (1973), Hubbard *et al* (1974) and Shawhan (1976). Nash (1979) suggested that variations with position in the surface conductivity of Io could strongly modulate these currents.

9.4. Interstellar dust

Watson (1972, 1973) has pointed out that photoemission from interstellar grains by galactic ultraviolet radiation can make a significant contribution to the heating of the interstellar gas. The rate of energy transfer from ultraviolet to gas kinetic energy depends on the grains's charge and can be comparable to heating by cosmic rays or x-rays. Photoemission alone can maintain gas temperatures near 50 K in 'standard' H I clouds.

The rate of growth and of coagulation of grains must depend upon their electric charge. This dependence has been considered by some workers (e.g. Salpeter and Watson 1973, Simpson *et al* 1979). A positive charge on grains will reduce the rate at which positive ions will attach to grains. However, either polarity of charge may enhance sticking rates of neutral molecules because of polarisation effects.

Several authors have speculated on the possibility of the acceleration of charged grains to very high velocities (Wickramasinghe 1972, 1974, Hayakawa 1976, Mendis and Wickramasinghe 1976). Grains expelled from cool stars at speeds of the order 10^8 cm s^{-1} might be accelerated to relativistic velocities by scattering off irregularities in the interstellar magnetic field (Dasgupta 1978, 1979). Hayakawa (1972) suggested that cosmic-ray air showers might be due to such grains, but this was disputed by Berezinsky and Prilutsky (1973).

Srnka and De (1978) noted that charge on a spinning grain gives a magnetic moment and internal magnetic field which may be larger than the external interstellar field. This could be important for aligning particles with the external magnetic field.

Finally, dust grains can provide a recombination surface for ions and electrons in the interstellar plasma which, in certain regions, can be competitive with ordinary radiative recombination (Snow 1975, Weisheit and Upham 1978) or with disassociative recombination or charge exchange rates in molecular clouds (Oppenheimer and Dalgarno 1974, Elmegreen 1979). The dust grains in this process also act as a catalyst to convert positive ions into neutrals.

10. Conclusions

The most significant result in this area of research in the last decade has undoubtedly been the discovery that large electrostatic potentials of the order of some tens of kV occur on objects in the solar system. The solar system is certainly not unique in this respect, nor is it a particularly exotic regime: there are regions with much hotter plasmas and with much larger magnetic fields. It is to be expected that the charging of objects in such regions will be correspondingly greater.

Electrostatic charging is certainly more important for some astrophysical processes than has been previously thought. One of the most significant applications may be in the condensation and coagulation process involving the growth of grains in interstellar clouds. This appears to be an area ripe for further theoretical and perhaps laboratory work.

The greatest deficiency at present is the lack of hard data on charging of natural objects such as dust grains. Direct measurement of charges on dust grains appears to be possible but no results have yet been reported. The development of additional observational tools is needed. The remote observation of discharges may be possible by means of light or radio noise detection. Active experiments should be considered, such as the release of dust in space followed by observation of its charging and motion, or artificial charging of dust on the lunar surface when lunar missions resume.

The physical processes involved in charging seem to be fairly well understood, at least qualitatively. The discipline will be put on a firmer quantitative basis with the current research programme that has been initiated. One drawback to quantitative work is that theoretical calculations of sheath structure and its effect on charging currents lean heavily on the use of large computer codes. It would be useful to have analytic approximations to some of the self-consistent numerical results, with quantities such as body size, Debye length, speed ratios, etc, entering as parameters.

Finally, large spacecraft with dimensions of the order of km are under consideration for future missions in space. Large structures such as solar power satellites can be particularly vulnerable to charging. Surfaces with large potentials such as solar arrays may be exposed to the plasma; the $\boldsymbol{V}\times\boldsymbol{B}$ induction effect increases with the size of a structure; both sunlight and magnetic shadowing effects are unavoidable. As a result we are seeing the development of a new engineering discipline: the electrical engineering of large systems in a plasma environment (Stevens 1980). A basic element in this discipline will be the physics of charging of surfaces in space.

Acknowledgments

I am grateful to a number of colleagues who have supplied preprints and unpublished data. I thank the following individuals for their comments on various parts of the manuscript: W Fillius, J G Laframboise, A D Mendis, R C Olsen, U Samir and P R Stannard. Much of my involvement in this area of research has been in collaboration with S E DeForest and L W Parker whose contributions to my own understanding I especially appreciate. I thank C E McIlwain for his support in general at UCSD and in particular through NASA Grant NGL 05-005-007. I also thank N J Stevens for his support through NASA Grant NAG 3-152. Partial support was also given through Air Force Contract FO4701-77-C-0062.

References

Aannestad P A and Purcell E M 1973 *Ann. Rev. Astron. Astrophys.* **11** 309–62

Aarset B, Cloud R W and Trump J G 1954 *J. Appl. Phys.* **25** 1365–8

Adamo R C and Nanevicz J E 1976 *Prog. Astron. Aeron.* **47** 225–35

Alfven H 1954 *On the Origin of the Solar System* (Oxford: Clarendon)

Allen J E, Boyd R L F and Reynolds P 1957 *Proc. Phys. Soc.* **70** 297–304

Al'pert J L 1965 *Space Sci. Rev.* **4** 373–415

Al'pert J L, Gurevic A V and Pitaevsky L P 1963 *Space Sci. Rev.* **2** 680–748

—— 1965 *Space Physics with Artificial Satellites* (New York: Consultants Bureau)

Arnoldy R L and Winckler J R 1981 *J. Geophys. Res.* **86** 575–84

Balmain K G 1979 *Spacecraft Charging Technology* ed R C Finke and C P Pike, AFGL-TR-79-0082 and NASA TM X-73537, pp 646–56

—— 1980 *Prog. Aeron. Astron.* **71** 276–98

Bartlett R O, DeForest S E and Goldstein R 1975 *AIAA 11th Electron Propulsion Conf., New Orleans* (New York: AIAA) AIAA Paper no 75-359

Bartlett R O and Purvis C K 1979 *Spacecraft Charging Technology* ed R C Finke and C P Pike, AFGL-TR-79-0082 and NASA TM X-73537, pp 44–58

Beard D B and Johnson F S 1960 *J. Geophys. Res.* **65** 1–7

—— 1961 *J. Geophys. Res.* **66** 4113–22

Beattie J R and Goldstein R 1977 *Proc. Spacecraft Charging Technology Conf.* ed C P Pike and R R Lovell, AFGL-TR-0051 and NASA TM X-73537, pp 144–66

Belton M J S 1966 *Science* **151** 35–44

Benson J 1977 *J. Geophys. Res.* **82** 1917–20

Berezinsky V S and Prilutsky O F 1973 *Astrophys. Space Sci.* **21** 475–6

Berg O, Richardson F F, Rhee J W and Auer S 1974 *Geophys. Res. Lett.* **1** 289–90

Berg O E, Wolf H and Rhee J 1975 *Interplanetary Dust and Zodiacal Light. Lecture Notes in Physics* **48** 233–7

Bering E A, Kelley M C, Mozer F S and Fahleson U V 1973 *Planet. Space Sci.* **21** 1983–2001

Bernstein I B and Rabinowitz I N 1959 *Phys. Fluids* **2** 112–21

Bertotti B 1961 *Phys. Fluids* **4** 1047–52

Besse A L and Rubin A G 1980 *J. Geophys. Res.* **85** 2324–8

Bettinger R T 1964 *An In Situ Probe System for the Measurement of Ionospheric Parameters. PhD Thesis* University of Maryland

Bohm D 1949 *The Characteristics of Electrical Discharges in Magnetic Fields* ed A Guthrie and R K Wakerling (New York: McGraw-Hill) chap 3

Bohm D, Burhop C H S and Massey H S W 1949 *The Characteristics of Electrical Discharges in Magnetic Fields* ed A Guthrie and R K Wakerling (New York: McGraw-Hill) chap 2

Bourdeau R E and Donley J L 1964 *Proc. R. Soc.* A **281** 487–504

Bourdeau R E, Donley J L, Serbu G P and Whipple E C 1961 *J. Astronaut. Sci.* **8** 65–73

Bowen P J, Boyd R L F, Henderson C L and Willmore A P 1964 *Proc. R. Soc.* A **281** 514–25

Brace L H 1981 unpublished data

Brace L H, Theis R F and Dalgarno A 1973 *Radio Sci.* **8** 341–8

Brownlee D E 1979 *Rev. Geophys. Space Phys.* **17** 1735–43

Brundin C L 1963 *AIAA J.* **11** 2529–37

Burke J R and Silk J 1974 *Astrophys. J.* **190** 1–10

Call S M 1969 *The Interaction of a Satellite with the Ionosphere. PhD Thesis, Rep. No 68* Columbia University, New York

Cauffman D P 1973a *Photon and Particle Interactions with Surfaces in Space* ed R J L Grard (Dordrecht: D Reidel) pp153–61

—— 1973b *Correlation of Strobe Anomalies with Geophysical Parameters. Aerospace Corporation, El Segundo, Tech. Memo. No* ATM-74(4409-04)-3

—— 1974 *A Study of IMP-6 Spacecraft Charging. Tech. Rep. Aerospace Corporation, El Segundo*

—— 1980 *Ionization and Attraction of Neutral Molecules to a Charged Spacecraft. Aerospace Corporation, El Segundo, Rep. No* SD-TR-80-78

Cauffman D P and Maynard N C 1974 *J. Geophys. Res.* **79** 2427–38

Cauffman D P and Shaw R R 1975 *Space Sci. Instrum.* **1** 125–37

Cernuschi F 1947 *Astrophys. J.* **105** 241–54

Chang HHC and Smith MC 1959 *J. Br. Interplanetary Soc.* **17** 199–205
Chang JS, Prokopenko SML, Godard R and Laframboise JG 1979 *Spacecraft Charging Technology* ed R C Finke and C P Pike, AFGL-TR-79-0082 and NASA Conf. Publ. 2071, pp179–96
Chang KW and Bienkowski GK 1970 *Phys. Fluids* **13** 902–20
Chappell CR, Baugher CR and Horwitz JL 1980 *Rev. Geophys. Space Phys.* **18** 853–61
Chen FF 1965a *J. Nucl. Energy* **C7** 47–67
—— 1965b *J. Appl. Phys.* **36** 675–8
Chen KM 1965 *Interaction of a Space Vehicle with an Ionized Atmosphere* ed S F Singer (Oxford: Pergamon) pp465–81
Chiu YT and Schulz M 1978 *J. Geophys. Res.* **83** 629–42
Chopra KP 1961 *Rev. Mod. Phys.* **33** 153–89
Cohen HA 1981 unpublished data
Cohen HA, Sherman C and Mullen EG 1979a *Geophys. Res. Lett.* **6** 515–8
Cohen HA, Sherman C, Mullen EG, Huber WB, Masek TD, Sluder RB, Mizera PF, Schnauss ER, Adamo RC, Nanevicz JE and Delorey DE 1979b *Spacecraft Charging Technology Conf.* ed CP Pike and R R Lovell, AFGL-TR-79-0082 and NASA Conf. Publ. 2071, pp80–90
Colligon JS 1961 *Vacuum* **11** 272–81
Consolmagno G 1979 *Icarus* **38** 398–410
—— 1980 *Nature* **285** 557–8
Cousinie P, Colombie N, Fert C and Simon R 1959 *C.R. Acad. Sci., Paris* **249** 387
Crawford FW and Harp RS 1965 *J. Geophys. Res.* **70** 587–96
Criswell DR 1973 *Photon and Particle Interactions with Surfaces in Space* ed R J L Grard (Dordrecht: D Reidel) pp545–56
Criswell DR and De BR 1977 *J. Geophys. Res.* **82** 1005–7
Darlington EH and Cosslett VE 1972 *J. Phys. D: Appl. Phys.* **5** 1969–81
Dasgupta AK 1978 *Astrophys. Space Sci.* **59** 347–54
—— 1979 *Astrophys. Space Sci.* **60** 455–64
Davis AH and Harris I 1961 *Rarefied Gas Dynamics* ed L Talbot (New York: Academic) pp691–9
De BR 1974 *Astrophys. Space Sci.* **30** 135–47
—— 1979 *J. Geophys. Res.* **84** 2655–6
De BR and Criswell DR 1977 *J. Geophys. Res.* **82** 999–1004
Decreau PME, Etcheto J, Knott K, Pedersen A, Wrenn GL and Young DT 1978 *Space Sci. Rev.* **22** 633–45
DeForest SE 1972 *J. Geophys. Res.* **77** 651–9
—— 1973 *Photon and Particle Interactions with Surfaces in Space* ed R J L Grard (Dordrecht: D Reidel) pp273–6
de Laszlo H 1932 *Phil. Mag.* **13** 1171–8
Dionne GF 1973 *J. Appl. Phys.* **44** 5361–4
—— 1975 *J. Appl. Phys.* **46** 3347–51
Draine BT 1978 *Astrophys. J. Suppl.* **36** 595–619
Draine BT and Salpeter EE 1979 *Astrophys. J.* **231** 77–94
Drell SD, Foley HM and Ruderman MA 1965a *Phys. Rev. Lett.* **14** 171–5
—— 1965b *J. Geophys. Res.* **70** 3131–45
Druyvesteyn MJ 1930 *Z. Phys.* **64** 781–98
DuBridge LA 1935 *New Theories of the Photoelectric Effect* (Paris: Hermann and Cie)
Durrett JC and Stevens JR 1979 *Spacecraft Charging Technology* ed R C Finke and C P Pike, AFGL-TR-79-0082 and NASA Conf. Publ. 2071, pp4–10
Elmegreen BG 1979 *Astrophys. J.* **232** 729–39
Everhart TE 1960 *J. Appl. Phys.* **31** 1483–90
Fahleson U 1973 *Photon and Particle Interactions with Surfaces in Space* ed R J L Grard (Dordrecht: D Reidel) pp563–9
Fechtig H, Grun E and Kissel J 1978 *Cosmic Dust* ed J A M McDonnell (New York: Wiley) pp607–69
Fechtig H, Grun E and Morfill G 1979 *Planet. Space Sci.* **27** 511–31
Fenner MA, Freeman JW and Hills HK 1973 *Proc. 4th Lunar Science Conf.* vol 3 (Oxford: Pergamon) pp2877–87
Feuerbacher B and Fitton B 1972 *J. Appl. Phys.* **43** 1563–72
Feuerbacher B, Willis RF and Fitton B 1973 *Astrophys. J.* **181** 101–13
Fillius W, McIlwain CE and Mogro-Campero A 1975 *Science* **188** 465–7
Fillius W, Ip WH and McIlwain CE 1980 *Science* **207** 425–31

Finke R C and Pike C P (ed) 1979 *Spacecraft Charging Technology* AFGL-TR-79-0082 and NASA Conf. Publ. 2071
Foti G, Potenza R and Triglia A 1974 *Lett. Nuovo Cim.* **11** 659
Fournier G 1971 *Collisionless Plasma Flow Around a Cylinder in View of Applications to Ionospheric Probes. PhD Thesis* Orsay
Fournier G and Pigache D 1975 *Phys. Fluids* **18** 1443–53
Fowler R H 1931 *Phys. Rev.* **38** 45–56
Fredricks R W and Scarf F L 1973 *Photon and Particle Interactions with Surfaces in Space* ed R J L Grard (Dordrecht: D Reidel) pp277–308
Freeman J W, Fenner M A and Hills H K 1973a *Photon and Particle Interactions with Surfaces in Space* ed R J L Grard (Dordrecht: D Reidel) pp363–8
—— 1973b *J. Geophys. Res.* **78** 4560–7
Fu J H M 1971 *J. Geophys. Res.* **76** 2506–9
Gail H P and Sedlmayr E 1975 *Astron. Astrophys.* **41** 359–66
Garrett H B 1979 *Spacecraft Charging Technology* ed R C Finke and C P Pike, AFGL-TR-79-0082 and NASA Conf. Publ. 2071, pp239–55
Garrett H B and DeForest S E 1979 *J. Geophys. Res.* **84** 2083–8
Gault D E, Adams J B, Collins R J, Kuiper G P, O'Keefe J A, Phinney R A and Shoemaker E M 1970 *Icarus* **12** 230–2
Gibbons D J 1966 *Handbook of Vacuum Physics* vol 2, Part 3, ed A H Beck (Oxford: Pergamon) pp301–95
Godard R 1975 *A Symmetric Model for Cylindrical and Spherical Collectors in a Flowing Collisionless Plasma. PhD Thesis* York University, Toronto
Gold T 1955 *Mon. Not. R. Astron. Soc.* **115** 585–604
—— 1961 *Space Astrophysics* ed W Liller (New York: McGraw-Hill) pp171–8
—— 1962 *The Moon* ed Z Kopal and Z K Mikhailov (New York: Academic) pp433–9
Gold T, Baron R L and Bilson E 1979 *Earth Planet. Sci. Lett.* **45** 133–40
Gold T and Williams G J 1973 *Photon and Particle Interactions with Surfaces in Space* ed R J L Grard (Dordrecht: D Reidel) pp557–60
Goldstein B 1974 *J. Geophys. Res.* **79** 23–35
Goldstein R and DeForest S E 1976 *Prog. Aeron. Astron.* **47** 169–81
Goldstein R and Divine N 1977 *Proc. Spacecraft Charging Technology Conf.* ed C P Pike and R R Lovell, AFGL-TR-0051 and NASA TM X-73537, pp131–41
Gonfalone A, Pedersen A, Fahleson U V, Falthammar C G, Mozer F S and Torbert R B 1979 *Spacecraft Charging Technology* ed R C Finke and C P Pike, AFGL-TR-0082 and NASA Conf. Publ. 2071, pp256–67
Grard R J L (ed) 1973a *Photon and Particle Interactions with Surfaces in Space* (Dordrecht: D Reidel)
—— 1973b *J. Geophys. Res.* **78** 2885–906
—— 1975 *Space Sci. Instrum.* **1** 363
—— 1976 *J. Geophys. Res.* **81** 1805–6
Grard R J L, DeForest S E and Whipple E C 1977 *Geophys. Res. Lett.* **4** 247–8
Gringauz K I 1963 *Planet. Space Sci.* **11** 281–96
Gringauz K I, Bezrukikh V V and Ozerov V D 1961 *Iskusstv. Sputniki Zemli* **6** 63–100
Gringauz K I and Zelikman M K 1957 *Usp. Fiz. Nauk* **63** 239–52
Grobman W D and Blank J L 1969 *J. Geophys. Res.* **74** 3943–51
Grun E 1980 *Proc. Halley Probe Plasma Environment Workshop, European Space Technical Center* ed R Reinhard (Nordwijk: ESTEC) ESA-SP 155
Guernsey R L and Fu J H M 1970 *J. Geophys. Res.* **75** 3193–9
Gurevich A V, Pitaevskii L P and Smirnova V V 1969 *Space Sci. Rev.* **9** 805–71
Gurnett D A 1972 *Astrophys. J.* **175** 525–33
Guth E and Mullin C J 1941 *Phys. Rev.* **59** 575–84
Habing H J 1968 *Bull. Astron. Inst. Netherlands* **19** 421–31
Hachenberg O and Brauer W 1959 *Adv. Electron. Electron Phys.* **11** 413–99
Hagstrum H D 1953 *Phys. Rev.* **89** 244–55
—— 1954 *Phys. Rev.* **96** 325–35
—— 1961 *Phys. Rev.* **123** 758–65
Hanson W B and Heelis R A 1975 *Space Sci. Instrum.* **1** 493–524
Hanson W B, Sanatani S and Hoffman J H 1981 *J. Geophys. Res.* to be published
Hanson W B, Sanatani S, Zuccaro D and Flowerday T W 1970 *J. Geophys. Res.* **75** 5483–501
Harp R S and Crawford F W 1964 *J. Appl. Phys.* **35** 3436–46

Hayakawa S 1972 *Astrophys. Space Sci* **16** 238–40
—— 1976 *Solid State Astrophysics* ed N C Wickramasinghe and D J Morgan (Dordrecht: D Reidel) pp93–9
Henderson C L and Samir U 1967 *Planet. Space Sci.* **15** 1499–513
Heroux L, Manson J E, Hinteregger H E and McMahon W J 1965 *J. Opt. Soc. Am.* **55** 103–4
Herring C and Nichols M H 1949 *Rev. Mod. Phys.* **21** 185–270
Hess W N, Trichel M C, Davis T N, Beggs W C, Kraft G E, Stassinopoulos E and Maier E J R 1971 *J. Geophys. Res.* **76** 6067–81
Hester S D and Sonin A A 1970 *Phys. Fluids* **13** 641–8
Hill A G, Buechner W W, Clark J S and Fisk J B 1939 *Phys. Rev.* **55** 463–70
Hill J R and Mendis D A 1979 *The Moon and the Planets* **21** 3–16
—— 1980 *The Moon and the Planets* **23** 53–71
—— 1981 *The Moon and the Planets* **24** 431–6
Hinteregger H E 1961 unpublished results
Hinteregger H E, Damon K R and Hall L A 1959 *J. Geophys. Res.* **64** 961–9
Hinteregger H E, Hall L A and Schmidtke G 1965 *Proc. 5th Int. Space Science Symp., Florence* ed D G King-Hele, P Muller and G Righini (Amsterdam: North-Holland) pp1175–90
Hinteregger H E and Watanabe K 1953 *J. Opt. Soc. Am.* **43** 604–8
Hoffmaster D K and Sellen J M 1976 *Prog. Astron. Aeron.* **47** 185–211
Hubbard R F, Shawhan S D and Joyce G 1974 *J. Geophys. Res.* **79** 920–8
Hughes D W 1980 *Nature* **283** 331–2
Humes D H, Alvarez J M, Kinard W H and O'Neal R L 1975 *Science* **188** 473–4
Illiano J M and Storey L R O 1974 *Planet. Space Sci.* **22** 873–8
Imyanitov I M 1957 *Usp. Fiz. Nauk* **63** 267–82
Inouye G T and Sellen J M 1978 *Effects of the Ionosphere on Space and Terrestrial Systems* ed J M Goodman (Washington, DC: US Government Printing Office) pp309–12
Ip W H 1979 *Nature* **280** 478–9
—— 1980 *Space Sci. Rev.* **26** 39–96
Israelson G A and Winckler J R 1979 *J. Geophys. Res.* **84** 1442–52
Jacobson T A and Maynard N C 1980 *Planet. Space Sci.* **28** 291–307
Jastrow R and Pearse C A 1957 *J. Geophys. Res.* **62** 413–23
Johnson B, Quinn J and DeForest S E 1978 *Effects of the Ionosphere on Space and Terrestrial Systems* ed J M Goodman (Washington, DC: US Government Printing Office) pp322–7
Johnson T V, Morfill G and Grun E 1980 *Geophys. Res. Lett.* **7** 305–8
Juenker D W, Waldron J P and Jaccodine R J 1965 *J. Opt. Soc. Am.* **54** 216–25
Jung B 1937 *Astron. Nach.* **263** 426
Kaminsky M 1965 *Atomic and Ionic Impact Phenomena on Metal Surfaces* (Berlin: Springer-Verlag)
Kanal M 1962 *Theory of Current Collection of Moving Spherical Probes. Space Physics Research Laboratory, University of Michigan, Ann Arbor, Sci. Rep. No* JS-5
Kasha M A 1969 *The Ionosphere and Its Interaction with Satellites* (New York: Gordon and Breach)
Katz I, Parks D E, Mandell M J, Harvey J M, Brownell D H, Wang S S and Rotenberg M 1977 *A Three Dimensional Dynamic Study of Electrostatic Charging in Materials* NASA CR-135256
Kawashima N 1972 *J. Geophys. Res.* **77** 6896–9
Knott K 1972 *Planet. Space Sci.* **20** 1137–46
—— 1973 *J. Geophys. Res.* **78** 3172–5
Knudsen W C 1966 *J. Geophys. Res.* **71** 4669–78
Knudsen W C and Harris K K 1973 *J. Geophys. Res.* **78** 1145–52
Knudsen W C and Sharp G W 1967 *J. Geophys. Res.* **72** 1061–72
Krasovskii V I 1958 *Iskusstv. Sputniki Zemli* **2** 36–49 (Engl. transl. 1961 *Planet. Space Sci.* **5** 223–32)
Kraus J D 1965 *Interactions of Space Vehicles with an Ionized Atmosphere* ed S F Singer (Oxford: Pergamon) pp325–72
Kurt P G and Moroz V I 1962 *Planet. Space Sci.* **9** 259–68
Laframboise J G 1966 *Theory of Spherical and Cylindrical Langmuir Probes in a Collisionless, Maxwellian Plasma at Rest. University of Toronto Institute for Aerospace Studies, Rep. No* 100
Laframboise J G and Parker L W 1973 *Phys. Fluids* **16** 629–36
Laframboise J G and Rubinstein J 1976 *Phys. Fluids* **19** 1900–8
Lam S H 1965a *Phys. Fluids* **8** 73–87
—— 1965b *Phys. Fluids* **8** 1002–4
Langmuir I and Blodgett K B 1923 *Phys. Rev.* **22** 347–56

—— 1924 *Phys. Rev.* **24** 49–59
Leadon R and Wilkenfeld J 1979 *Spacecraft Charging Technology* ed R C Finke and C P Pike, AFGL-TR-79-0082 and NASA Conf. Publ. 2071, pp704–10
Lehn WL 1977 *Proc. Spacecraft Charging Technology Conf.* ed C P Pike and R R Lovell, AFGL-TR-0051 and NASA TM X-73537, pp559–67
Lehnert B 1956 *Tellus* **8** 408–9
Liemohn HB 1976 *Electrical Charging of Shuttle Orbiter. Battelle Pacific Northwest Laboratory Rep. No* BN SA 518, Richland
—— 1977 *Proc. Spacecraft Charging Technology Conf.* ed C P Pike and R R Lovell, AFGL-TR-0051 and NASA TM X-73537, pp271–86
Lindeman R, Freeman J W and Vondrak R R 1973 *Proc. 4th Lunar Science Conf.* vol 3 (Oxford: Pergamon) pp2889–96
Linson L M 1969 *J. Geophys. Res.* **74** 2368–74
Liu V C 1969 *Space Sci. Rev.* **9** 423–90
Liu V C and Hung R J 1968 *Planet. Space Sci.* **16** 845–62
Liu V C and Jew H 1968 *AIAA Sixth Aerospace Sci. Meeting, New York* (New York: AIAA) AIAA Paper no 68–169
Lovell R R, Stevens N J, Schober W, Pike C P and Lehn W 1976 *Prog. Astron. Aeron.* **47** 3–14
Lukirskii A P, Rumsh M A and Smirnov L A 1960 *Opt. Spectrosc.* **9** 265–7
McAfee W S 1976 *J. Appl. Phys.* **47** 1179–84
McCoy J E and Criswell D R 1974 *Proc. 5th Lunar Science Conf.* vol 3 (Oxford: Pergamon) pp2991–3005
McCracken G M 1975 *Rep. Prog. Phys.* **38** 241–327
McDonnell J A M 1978 *Cosmic Dust* ed J M McDonnell (New York: Wiley) pp337–426
McGuire R E 1972 *Cosmic Electrodyn.* **3** 208–39
McPherson D A, Cauffman D P and Schober W R 1975 *J. Spacecraft and Rockets* **12** 621–6
McPherson D A and Schober W R 1976 *Prog. Astron. Aeron.* **47** 15–30
Makita H and Kuriki K 1978 *Phys. Fluids* **21** 1279–86
Malter L 1936 *Phys. Rev.* **50** 48–58
Mandell M J, Katz I, Schnuelle G W, Steen P G and Roche J C 1978 *IEEE Trans. Nucl. Sci.* **NS-25** 1–13
Manka R H 1972 *Lunar Atmosphere and Ionosphere. PhD Thesis* Rice University, Houston
—— 1973 *Photon and Particle Interactions with Surfaces in Space* ed R J L Grard (Dordrecht: D Reidel) pp347–61
Manka R H and Michel F C 1973 *Proc. 4th Lunar Science Conf.* vol 3 (Oxford: Pergamon) pp2897–908
Mendis D A 1979 *Astrophys. Space Sci.* **65** 5–12
—— 1981 *The Role of Electrostatic Charging of Small and Intermediate Sized Bodies in the Solar System* ed F D Kahn (Dordrecht: D Reidel)
Mendis D A and Axford W I 1974 *Ann. Rev. Earth Planet. Sci.* **2** 419–74
Mendis D A, Hill J R, Houpis H L F and Whipple E C 1981 *Astrophys. J.* to be published
Mendis D A and Wickramasinghe N C 1976 *Astrophys. Space Sci.* **42** L11–5
Meulenberg A 1976 *Prog. Astron. Aeron.* **47** 237–46
Mizera P F, Schnauss E R, Vandre R and Mullen E G 1979 *Spacecraft Charging Technology* ed R C Finke and C P Pike, AFGL-TR-79-0082 and NASA Conf. Publ. 2071, pp91–100
Montgomery M D, Asbridge J R, Bame S J and Hones E W 1973 *Photon and Particle Interactions with Surfaces in Space* ed R J L Grard (Dordrecht: D Reidel) pp247–61
Moorwood A F M and Feuerbacher B 1976 *Solid State Astrophysics* ed N C Wickramasinghe and D J Morgan (Dordrecht: D Reidel) pp179–89
Morfill G E and Grun E 1979a *Planet. Space Sci.* **27** 1269–82
—— 1979b *Planet Space Sci.* **27** 1283–92
Morfill G E, Grun E and Johnson T V 1980a *Planet. Space Sci.* **28** 1087–100
—— 1980b *Planet. Space Sci.* **28** 1101–10
—— 1980c *Planet. Space Sci.* **28** 1111–4
—— 1980d *Planet. Space Sci.* **28** 1115–23
Morrison P J, Thompson W B, Williamson P R 1978 *IEEE Trans. Plasma Sci.* **PS-6** 435–41
Nanevicz J E and Adamo R C 1976 *Prog. Astron. Aeron.* **47** 247–61
Nash D B 1979 *J. Geophys. Res.* **84** 5302–10
Nawrocki P J and Papa R 1961 *Atmospheric Processes. Air Force Cambridge Research Laboratory Rep.* 595
Norman K and Freeman R M 1973 *Photon and Particle Interactions with Surfaces in Space* ed R J L Grard (Dordrecht: D Reidel) pp231–44
Ogilvie K W, Scudder J D, Vasyliunas V M, Hartle R H and Siscoe G L 1977 *J. Geophys. Res.* **82** 1807–24

Olsen R C 1980 *Differential and Active Charging Results from the ATS Spacecraft. PhD Thesis* University of California at San Diego
Olsen R C, McIlwain C E and Whipple E C 1981 *J. Geophys. Res.* **86** 6809–19
Olsen R C and Purvis C K 1981 *J. Geophys. Res.* submitted
Opik E J 1957 *Irish Astron. J.* **4** 84–135
—— 1962 *Planet. Space Sci.* **9** 211–44
—— 1965 *Interaction of Space Vehicles with an Ionized Atmosphere* ed S F Singer (Oxford: Pergamon) pp3–60
Opik E J and Singer S F 1960 *J. Geophys. Res.* **65** 3065–70
Oppenheimer M and Dalgarno A 1974 *Astrophys. J.* **192** 29–32
Oran W A, Stone N H and Samir U 1975 *J. Geophys. Res.* **80** 207–9
Parker E N 1964 *Astrophys. J.* **139** 951–9
Parker J H 1954 *Phys. Rev.* **93** 1148–56
Parker L W 1964 *Numerical Methods for Computing the Density of a Rarefied Gas About a Moving Object. AFGL Rep.* 64–193
—— 1973 *Computer Solutions in Electrostatic Probe Theory I. Spherical Symmetry with Collisions. Air Force Avionics Laboratory Rep.* TR-72-222, Part I
—— 1976a *Computation of Collisionless Steady-State Plasma Flow Past a Charged Disk.* NASA CR-144159
—— 1976b *Theory of Electron Emission Effects in Symmetric Probe and Spacecraft Sheaths. AFGL Rep.* TR-76-024
—— 1978 *J. Geophys. Res.* **83** 4873–6
—— 1980 *Prog. Astron. Aeron.* **71** 477–522
Parker L W and Murphy B L 1967 *J. Geophys. Res.* **72** 1631–6
Parker L W and Oran W A 1979 *Spacecraft Charging Technology* ed R C Finke and C P Pike, AFGL-TR-79-0082 and NASA Conf. Publ. 2071, pp376–87
Parker L W and Whipple E C 1967 *Ann. Phys., NY* **44** 126–61
—— 1970 *J. Geophys. Res.* **75** 4720–33
Parks D E and Katz I 1981 *Proc. 3rd Spacecraft Charging Conf.* ed C P Pike and N J Stevens (Bedford, Mass.: Air Force Geophysics Laboratory) to be published
Parthasarathy R 1978 *Astron. J.* **83** 1235–9
Peale S J 1966 *J. Geophys. Res.* **71** 911–33
Pike C P and Bunn M M 1976 *Prog. Astron. Aeron.* **47** 45–60
Pike C P and R R Lovell (ed) 1977 *Proc. Spacecraft Charging Technology Conf.* AFGL-TR-0051 and NASA TM X-73537
Pike C P and Stevens N J (ed) 1981 *Proc. 3rd Spacecraft Charging Conf.* (Bedford, Mass.: Air Force Geophysics Laboratory) to be published
Prokopenko S M L and Laframboise J G 1977 *Proc. Spacecraft Charging Technology Conf.* ed C P Pike and R R Lovell, AFGL-TR-0051 and NASA TM X-73537, pp369–87
—— 1980 *J. Geophys. Res.* **85** 4125–31
Purvis C K 1980 *Configuration Effects on Satellite Charging Response. 18th Aerospace Sciences Meeting, Pasadena* (New York: AIAA) AIAA Paper no 80–0040
Purvis C K and Bartlett R O 1980 *Prog. Astron. Aeron.* **71** 299–317
Purvis C K, Bartlett R O and DeForest S E 1977 *Proc. Spacecraft Charging Technology Conf.* ed C P Pike and R R Lovell, AFGL-TR-0051 and NASA TM X-73537, pp107–20
Rawer K 1963 *Radio Astronomical and Satellite Studies of the Atmosphere* ed J Aarons (Amsterdam: North-Holland) pp385–99
Reasoner D L and Burke W J 1972 *J. Geophys. Res.* **77** 6671–87
—— 1973 *Photon and Particle Interactions with Surfaces in Space* ed R J L Grard (Dordrecht: D Reidel) pp369–87
Reasoner D L, Lennartsson W and Chappell C R 1976 *Prog. Astron. Aeron.* **47** 89–101
Reiff P H 1976 *J. Geophys. Res.* **81** 3423–7
Reiff P H, Freeman J W and Cooke D L 1979 *Prog. Astron. Aeron.* **71** 554–76
Rennilson J J and Criswell D R 1974 *The Moon* **10** 121–42
Rentschler H C, Henry D E and Smith K O 1931 *Rev. Sci. Instrum.* **3** 794–802
Rhee J W 1967 *The Zodiacal Light and the Interplanetary Medium* ed J L Weinberg, NASA SP-150, pp291–8
—— 1976 *Interplanetary Dust and Zodiacal Light. Lecture Notes in Physics* **48** 238–40
Robinson P A and Holman A B 1977 *Proc. Spacecraft Charging Technology Conf.* ed C P Pike and R R Lovell, AFGL-TR-0051 and NASA TM X-73537, pp297–308

Rosen A (ed) 1976 *Prog. Astron. Aeron.* **47** (Cambridge, Mass.: MIT Press)
Rosenbauer H R 1973 *Photon and Particle Interactions with Surfaces in Space* ed R J L Grard (Dordrecht: D Reidel) pp139–51
Rubin A G, Rothwell P L and Yates G K 1978 *Effect of the Ionosphere on Space and Terrestrial Systems* ed J M Goodman (Washington, DC: US Government Printing Office) pp313–5
Rubinstein J and Laframboise J G 1978 *Phys. Fluids* **21** 1655–6
Rumsh M A, Lukirskii A P and Schemelev V N 1960 *Sov. Phys.–Dokl.* **5** 1231–3
Sagalyn R C and Burke W J 1977 *Proc. Spacecraft Charging Technology Conf.* ed C P Pike and R R Lovell, AFGL-TR-0051 and NASA TM X-73537, pp67–79
Salpeter E E and Watson W D 1973 *Interstellar Dust and Related Topics* ed J M Greenberg and H C Van de Hulst (Dordrecht: D Reidel) pp363–7
Samir U 1970 *J. Geophys. Res.* **75** 855–8
—— 1973 *Photon and Particle Interactions with Surfaces in Space* ed R J L Grard (Dordrecht: D Reidel) pp193–219
Samir U, First M, Maier E J and Troy B 1975 *J. Atmos. Terr. Phys.* **37** 577–86
Samir U, Gordon R, Brace L and Theis R 1979 *J. Geophys. Res.* **84** 513–25
Samir U and Jew H 1972 *J. Geophys. Res.* **77** 6819–27
Samir U, Kaufman Y J, Brace L H and Brinton H C 1980 *J. Geophys. Res.* **85** 1769–72
Samir U and Willmore A P 1965 *Planet. Space Sci.* **13** 285–96
—— 1966 *Planet. Space Sci.* **14** 1131–7
Samir U and Wrenn G L 1969 *Planet. Space Sci.* **17** 693–706
—— 1972 *Planet. Space Sci.* **20** 899–904
Samson J A R and Cairns R B 1965 *Rev. Sci. Instrum.* **36** 19–21
Sanders N L and Inouye G T 1978 *Effect of the Ionosphere on Space and Terrestrial Systems* ed J M Goodman (Washington, DC: US Government Printing Office) pp285–92
Sanmartin J R 1970 *Phys. Fluids* **13** 103–16
Scarf F L 1975 *The Magnetospheres of the Earth and Jupiter* ed V Formisano (Dordrecht: D Reidel) pp433–49
—— 1976 *Jupiter* ed T Gehrels (Tucson: University of Arizona Press) pp870–95
Scarf F L, Fredricks R W, Green I M and Crook G M 1974 *J. Geophys. Res.* **79** 73–86
Schroder H 1973 *Photon and Particle Interactions with Surfaces in Space* ed R J L Grard (Dordrecht: D Reidel) pp51–8
Scudder J D, Sittler E C and Bridge H S 1981 *J. Geophys. Res.* to be published
Shapiro II, Lautman D A and Colombo G 1966 *J. Geophys. Res.* **71** 5695–704
Shaw R R, Nanevicz J E and Adamo R C 1976 *Prog. Astron. Aeron.* **47** 61–76
Shawhan S D 1976 *J. Geophys. Res.* **81** 3373–9
Shawhan S D, Hubbard R E, Joyce G and Gurnett D A 1973 *Photon and Particle Interactions with Surfaces in Space* ed R J L Grard (Dordrecht: D Reidel) pp405–13
Shen C S and Chopra K P 1963 *J. Atmos. Sci.* **20** 359–65
Shimizu R 1974 *J. Appl. Phys.* **45** 2107–11
Shkarofsky I P 1971 *J. Geophys. Res.* **76** 3746–54
Simon A 1955 *Phys. Rev.* **98** 317–8
Simons S 1976a *Astrophys. Space Sci.* **41** 423–34
—— 1976b *Astrophys. Space Sci.* **41** 435–45
Simpson I C, Simons S and Williams I P 1978 *Astrophys. Space Sci.* **59** 389–411
—— 1979 *Astrophys. Space Sci.* **61** 65–80
Singer S F 1956 *Scientific Uses of Earth Satellites* ed J A Van Allen (Ann Arbor: University of Michigan Press) pp304–16
Singer S F (ed) 1965 *Interaction of Space Vehicles with an Ionized Atmosphere* (Oxford: Pergamon)
Singer S F and Walker E H 1962a *Icarus* **1** 7–12
—— 1962b *Icarus* **1** 112–20
Smith B A *et al* 1979 *Science* **204** 951–72
Snow T P 1975 *Astrophys. J. Lett.* **202** L87–90
Soop M 1972 *Planet. Space Sci.* **20** 859–70
—— 1973 *Photon and Particle Interactions with Surfaces in Space* ed R J L Grard (Dordrecht: D Reidel) pp127–36
Spitzer L 1941 *Astrophys. J.* **93** 369–79
—— 1948 *Astrophys. J.* **107** 6–33
Spitzer L and Savedoff M P 1950 *Astrophys. J.* **111** 593–608

Srnka L J and De B R 1978 *Astrophys. J.* **225** 422–6
Stevens N J 1980 *Prog. Aeron. Astron.* **71** 437–76
Stone N H, Samir U and Wright K H 1978 *J. Geophys. Res.* **83** 1668–72
Suhrmann R and Pietrzyk J 1944 *Z. Phys.* **122** 600–13
Swift J D and Schwar M J R 1970 *Electrical Probes for Plasma Diagnostics* (London: Iliffe)
Takayama K, Ikegami H and Miyazaki S 1960 *Phys. Rev. Lett.* **5** 238–40
Taylor J C 1967 *Planet. Space Sci.* **15** 155–87
Troy B E, Maier E J and Samir U 1975 *J. Geophys. Res.* **80** 993–7
Tunaley J K E and Jones J 1973 *Photon and Particle Interactions with Surfaces in Space* ed R J L Grard (Dordrecht: D Reidel) pp59–71
Vedder J F 1966 *Rev. Space Sci.* **6** 365–414
Vogl J L, Sanders N L and DeForest S E 1976 *Prog. Astron. Aeron.* **47** 77–88
Walbridge E H 1969 *Icarus* **10** 342–3
Walker E H 1964 *Plasma Sheath and Screening Around a Stationary Charged Sphere and a Rapidly Moving Charged Body. PhD Thesis* University of Maryland, College Park
—— 1965 *Interactions of Space Vehicles with an Ionized Atmosphere* ed S F Singer (Oxford: Pergamon) pp61–162
Walker W C, Wainfan N and Weissler G L 1955 *J. Appl. Phys.* **26** 1366–71
Warner A H 1931 *Phys. Rev.* **38** 1871–5
Warwick J W *et al* 1981 *Science* **212** 239–43
Watson W D 1972 *Astrophys. J.* **176** 103–10
—— 1973 *Interstellar Dust and Related Topics. IAU Symp.* 52 ed J M Greenberg and H C Van de Hulst (Dordrecht: D Reidel) pp335–9
Weisheit J C and Upham R J 1978 *Mon. Not. R. Astron. Soc.* **184** 227–34
Wesson P S 1974 *Space Sci. Rev.* **15** 469–82
Whale H A 1964 *J. Geophys. Res.* **69** 447–56
Whipple E C 1965 *The Equilibrium Electric Potential of a Body in the Upper Atmosphere and in Interplanetary Space. PhD Thesis* The George Washington University, Washington, DC
—— 1976a *J. Geophys. Res.* **81** 715–9
—— 1976b *J. Geophys. Res.* **81** 601–7
—— 1977 *Proc. Spacecraft Charging Technology Conf.* ed C P Pike and R R Lovell, AFGL-TR-0051 and NASA TM X-73537, pp225–35
Whipple E C and Parker L W 1969a *J. Geophys. Res.* **74** 2962–71
—— 1969b *J. Geophys. Res.* **74** 5763–74
Whipple E C, Warnock J M and Winkler R H 1974 *J. Geophys. Res.* **79** 179–86
Whipple F L 1940 *Proc. Am. Phil. Soc.* **83** 711–45
—— 1960 *Physics and Medicine of the Atmosphere and Space* ed O O Benson and H Strughold (New York: Wiley) pp48–59
Wickramasinghe N C 1972 *Mon. Not. R. Astron. Soc.* **159** 269–87
—— 1974 *Astrophys. Space Sci.* **28** L25–9
Williamson P R and Banks P M 1976 *The tethered balloon current generator—a space shuttle-tethered subsatellite for plasma studies and power generation. National Oceanographic and Atmospheric Administration Final Rep., Boulder, Colorado*
Willis R F, Anderegg M, Feuerbacher B and Fitton B 1973a *Photon and Particle Interactions with Surfaces in Space* ed R J L Grard (Dordrecht: D Reidel) pp389–401
Willis R F, Feuerbacher B and Fitton B 1973b *Interstellar Dust and Related Topics. IAU Symp. 52* ed J M Greenberg and H C Van de Hulst (Dordrecht: D Reidel) pp303–9
Winckler J R 1980 *Rev. Geophys. Space Phys.* **18** 659–82
Wrenn G L 1979 *Nature* **277** 11–2
Wrenn G L and Heikkila W J 1973 *Photon and Particle Interactions with Surfaces in Space* ed R J L Grard (Dordrecht: D Reidel) pp221–30
Wrenn G L, Johnson J F E and Sojka J J 1979a *Nature* **279** 512–4
Wrenn G L, Johnstone A D and Johnson J F E 1979b *Spacecraft Charging Studies in Europe. Air Force Office of Scientific Studies Final Rep. Grant No* AFOSR-78-3713
Wyatt S P 1969 *Planet. Space Sci.* **17** 155–71
Yadlowsky E J, Hazelton R C and Churchill R J 1979 *Spacecraft Charging Technology* ed R C Finke and C P Pike, AFGL-TR-79-0082 and NASA Conf. Publ. 2071, pp632–45
Yanagita S 1977 *Astrophys. Space Sci.* **49** L11–5